BL5U

Topological Phase Transition in Ultrathin Bi Films on Bi_2Te_3 Substrates

T. Hirahara[1], M. Aitani[1], M. Yamada[1], H. Miyazaki[2], M. Matsunami[2], S. Kimura[2] and S. Hasegawa[1]

[1]*Department of Physics, University of Tokyo, 7-3-1 Hongo, Bunkyo-ku, Tokyo 113-0033, Japan*
[2]*UVSOR Facility, Institute for Molecular Science, Okazaki 444-8585, Japan*

Topological insulators have become one of the model systems to study Dirac physics in solids. They are mathematically characterized by the Z_2 topological number with edge modes that cannot be backscattered [1]. An essential ingredient in realizing a topological insulator is the parity inversion induced by the strong spin-orbit coupling. From this viewpoint, bismuth (Bi), which is virtually the heaviest nonradioactive element, has been the main building block. Nowadays many Bi alloys are known as topological insulators. Although it is necessary to make alloys, inhomogeneity may be introduced in the grown samples. Therefore, searching for other ways to produce novel topological materials with simple, well-defined structures is important.

In this respect, driving a quantum topological phase transition [making a normal (trivial) material into a topological (nontrivial) one] in a simple system seems to be a rather smart approach. One example of such a transition is the case of Bi, where the three-dimensional (3D) trivial bulk becomes topological in two dimensions by making thin films of 1–8 bilayers (BL) [2, 3]. Another way to induce a topological phase transition is to apply pressure and change the lattice parameters slightly, which is experimentally not easy to do.

In this study, we have attempted to change the lattice constant by growing an ultrathin film. We have fabricated Bi films on Bi_2Te_3 substrates and measured the band dispersion with angle-resolved photoemission spectroscopy. Due to the small in-plane lattice mismatch between Bi and Bi_2Te_3 (~3.6 %), Bi can be grown epitaxially on Bi_2Te_3 from 1 BL [4]. Figure 1(a) shows the band dispersion of a 7 BL Bi film on Bi_2Te_3. Compared to the 7 BL Bi film grown on Si(111)-7x7 [Fig. 1(b)], the band dispersion is significantly different near the Γ point.

The change in the band dispersion of the Bi films shown in Fig. 1 can be explained by the change in the lattice constant. Our detailed LEED-IV measurements showed that due to the contraction of the in-plane lattice contraction by ~3.6 %, the out-of-plane lattice constant is expanded ~4 % [5]. The Poisson ratio, which is the ratio of the above two changes is as large as 1, meaning a very large distortion. We have further found that the lattice constant returns back to its original bulk value at ~15 BL.

The band dispersion in Fig. 1(a) is reproduced by *ab initio* calculations for a free standing Bi slab when the experimentally obtained lattice parameters are used. Furthermore, by calculating the 3D Z_2 topological for this strained Bi, we have found that the originally trivial Bi becomes nontrivial. Thus it is shown that the topological properties of Bi can be changed by inducing a small change in the lattice parameters [5].

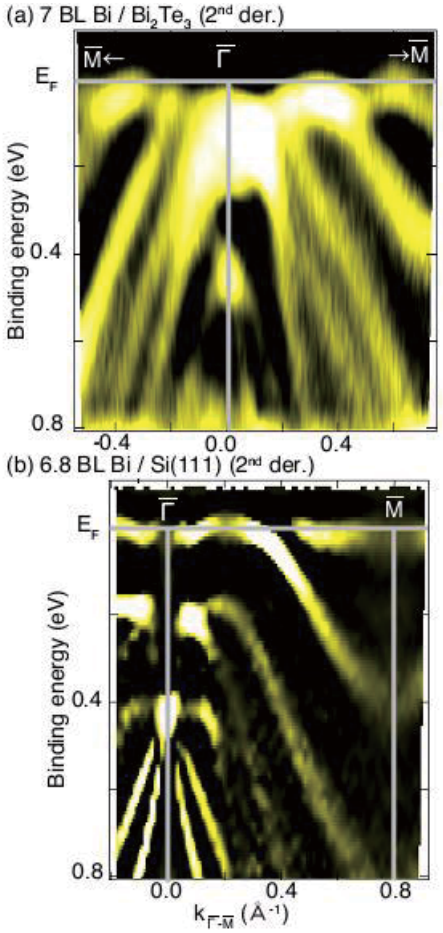

Fig. 1. The band dispersion of a 7 BL Bi(111) film grown on Bi_2Te_3 (a), and that on Si(111) (b).

[1] M. Z. Hasan and C. L. Kane, Rev. Mod. Phys. **82** 3045 (2010).
[2] S. Murakami, Phys. Rev. Lett. **97** (2006) 236805
[3] Z. Liu *et al*., Phys. Rev. Lett. **107** (2011) 136805.
[4] T. Hirahara *et al.,* Phys. Rev. Lett. **107** (2011) 166801.
[5] T. Hirahara *et al.,* Phys. Rev. Lett. **109** (2012) 227401.

Hydrogen Reduction of Pd Catalysts Studied by Transmission Soft-X-Ray Absorption Spectroscopy

H. Kondoh[1,2], R. Toyoshima[1], K. Suzuki[1], M. Yoshida[1], H. Yuzawa[2], M. Nagasaka[2] and N. Kosugi[2]

[1]*Department of Chemistry, Keio University, Yokohama 223-8522, Japan*

[2]*Department of Photo-Molecular Science, Institute for Molecular Science, Okazaki 444-8585, Japan*

Hydrogenation of unsaturated hydrocarbon is one of key reactions both in the fundamental organosynthesis and in the chemical industry. Pd nanoparticles supported on amorphous carbon are well known as good catalysts for hydrogenation using atmospheric H_2 gas. Also Pd has a capability to absorb hydrogen in the bulk. Recently it was demonstrated that the absorbed hydrogen has a close relation to the catalytic activity for the hydrogenation of unsaturated hydrocarbon at the surfaces [1]. Furthermore, carbonaceous species included in the Pd catalysts give significant effects on the hydrogen absorption and hence on the hydrogenation activity. The oxidation state of Pd should be also important to the activity. However, chemical behavior of the Pd catalysts has been hardly observed under gas flow conditions. In this work, we studied Pd nanoparticles and Pd porous films from the viewpoint of chemical state of oxygen adsorbed on and/or included in the Pd catalysts under atmospheric H_2 gas flow conditions by means of transmission soft-x-ray absorption spectroscopy.

Transmission NEXAFS spectra were measured at BL3U using a photodiode detector mounted in He path [2]. The Pd nanoparticles were supported on amorphous carbon and the hydrogenation activity was checked for butene at 295 K with a flow cell and mass spectrometry. The Pd porous film was prepared by temporal immersion of a Pd foil into aqua regia and subsequent rinses with pure water and acetone. These Pd catalysts were loaded in the flow cell with a sandwiched configuration between two Si_3N_4 windows of 100 nm thickness.

O K-edge transmission NEXAFS spectra for the Pd nanoparticles supported on amorphous carbon were taken at 295 K before and under H_2 flow as shown in Fig. 1. Before H_2 flow, several peaks (A-D) are observed at a lower energy range from 532 to 538 eV, which are tentatively associated with adsorbed O-containing species on the Pd surfaces and surface oxides of Pd nanoparticles, while under H_2 flow these peaks diminish significantly. This decrease in intensity indicates reduction and removal of the O-containing surface species under H_2 flow even at room temperature. A prominent and broad peak is observed at around 540 eV. This peak is attributed to oxygen atoms of a Pd oxide included in the particles. This oxide peak does not disappear even under H_2 flow, which suggests that the Pd oxide included in the particles is not reduced even under hydrogen-rich conditions. A similar trend was observed for a Pd porous film as shown in Fig. 2: The low-energy peaks (A-D) almost disappear, while main structures at 540 eV and 550-560 eV remain under H_2 flow.

The next step is in-situ monitoring of behavior of included carbon as well as included oxygen under hydrogenation reaction conditions, which will reveal the relation between the presence of carbon and oxygen in the Pd catalysts and the hydrogenation activity.

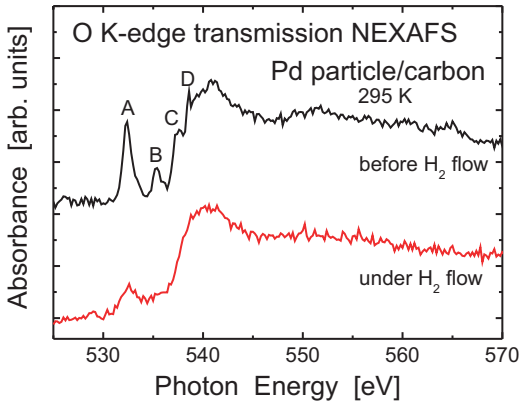

Fig. 1. O-K transmission NEXAFS spectra taken for Pd nanoparticles supported on amorphous carbon before (upper) and under (lower) H_2 gas flow (200 SCCM).

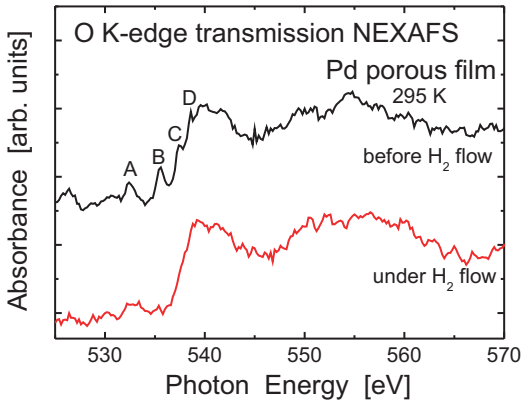

Fig. 2. O-K transmission NEXAFS spectra taken for a Pd porous film before (upper) and under (lower) H_2 gas flow (200 SCCM).

[1] M. Wilde *et al.,* Angew. Chem. Int. Ed. **47** (2008) 9289.

[2] M. Nagasaka *et al*., J. Electron. Spectrosc. Relat. Phenom. **177** (2010) 130.

BL3U

The Study on Nickel-Borate Oxygen Evolution Catalyst by Soft X-ray Electrochemical XAFS

M. Yoshida[1], T. Mineo[1], T. Yomogida[1], H. Yuzawa[2], M. Nagasaka[2], N. Kosugi[2] and H. Kondoh[1,2]

[1]*Department of Chemistry, Keio University, Yokohama 223-8522, Japan*
[2]*Department of Photo-Molecular Science, Institute for Molecular Science, Okazaki 444-8585, Japan*

Electrochemical water splitting to hydrogen and oxygen gases is an attractive and promising approach toward highly efficient energy conversion. This reaction is derived from two half reactions of hydrogen evolution reaction (HER) and oxygen evolution reaction (OER). However, many electrode materials are known to be not active for OER due to the high overpotentials. Recently, a nickel-borate thin film was reported as an efficient electrocatalyst for OER [1]. The local structure around the nickel ions of this thin film was revealed by Ni K-edge XAFS measurements, while that around B species is still unclear. The structure and chemical state of the B species may change depending on the film growth. Thus, in this study, the nickel-borate thin film were investigated by B K-edge XAFS measurements under potential control conditions.

The soft X-ray electrochemical XAFS measurements were performed with the transmission mode at BL3U of UVSOR, according to the previous work [2]. Au/Cr/Si_3N_4 thin film substrates were used as working electrodes. A home-made electrochemical cell was used with a Pt mesh counter electrode and a Ag/AgCl (saturated KCl) reference electrode in a potassium borate aqueous solution.

Figure 1 shows B K-edge XAFS spectra taken for nickel-borate thin film electrodeposited at 2.0 V vs Ag/AgCl. Prominent peaks associated with B species were observed at ca. 192 eV. The peak positions were slightly different between the samples before and after cyclic voltammetry measurements, indicating that the chemical state of B in the nickel-borate thin film is likely to change by potential control.

In-situ B K-edge XAFS spectra for the nickel-borate deposition on the Au/Cr/Si_3N_4 electrode were measured as a function of time in a potassium borate aqueous solution containing nickel nitrate at 0.9 V, as shown in Fig. 2. A broad peak grows gradually at ca. 192 eV, suggesting that the nickel-borate thin film was deposited on the Au/Cr/Si_3N_4 electrode. The B species at the solid-liquid interface was successfully detected under potential control for the first time by the in-situ B K-edge XAFS measurement. This in-situ technique will be applied to investigation of structures and chemical states of nickel-borate thin films under working conditions as the OER electrocatalyst.

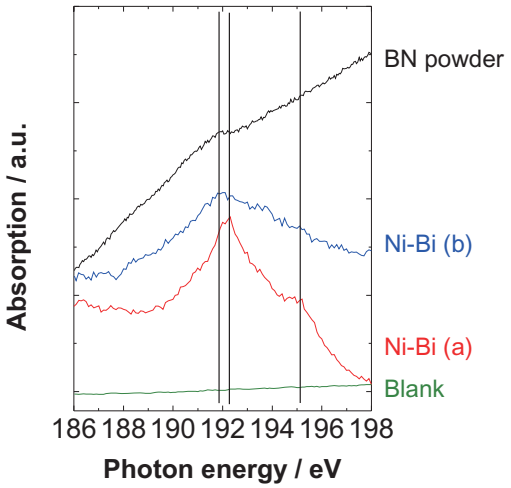

Fig. 1. B K-edge XAFS spectra taken for the nickel-borate thin film and BN powder reference. The samples were measured before (a) and after (b) cyclic voltammetry.

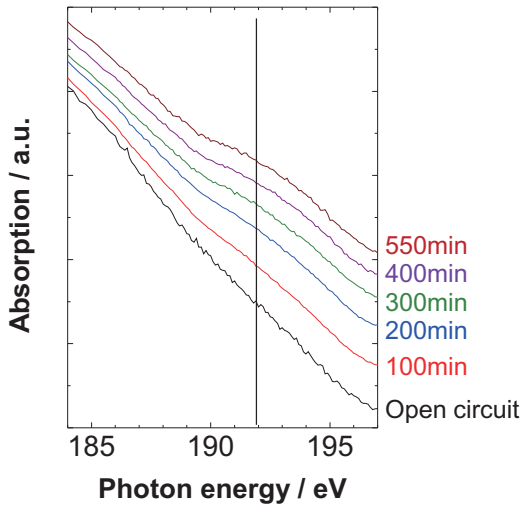

Fig. 2. Time course of in-situ B K-edge XAFS spectra during electrodeposition of nickel-borate thin film.

[1] D. K. Bediako *et al.*, J. Am. Chem. Soc. **134** (2012) 6801.
[2] M. Nagasaka *et al.*, J. Electron. Spectrosc. Relat. Phenom. **177** (2010) 130.

BL3B

Photoionization Threshold Measurement of Porphyrin Derivatives at the Surface of Water

T. Ishioka, K. Tomita, T. Morimoto and A. Harata

Molecular and Material Sciences, Kyushu University, Kasuga, Fukuoka 816-8580, Japan

Porphyrin derivatives play import roles in natural science such as photosynthesis and energy transfer systems in a cell. A number of research works have been carried out utilizing the ring molecule for converting photon energy to chemical structure [1]. In such cases, porphyrin molecules are usually dissolved into some kinds of solvents. Wavelength regions effective for reactions are limited by light absorption of the solvents. Water surfaces are ideal environments for utilizing photon energies since loss of photon energy can be minimized. Moreover, source molecules for chemical synthesis are easily supplied from both gas phase and solution. However, physical and chemical properties of such photoactive molecules are usually known for gas phase or solution phase. The properties of surface phase are not easily accessible, which are essential for designing photoinduced reactions at the surface. In this work, photoionization behavior of porphyrin derivatives has been analyzed by utilizing synchrotron light source. Solvation state of such molecules at the surface of water are also discussed by comparing the determined threshold values to those in vacuum.

In a typical photoionization measurement, monochromated light was emitted from the chamber to a He-purged cell through an MgF_2 window. The range of light energy was in 4-8 eV. The emitted light was reflected with an Al mirror and vertically irradiated on the sample surface. High voltage (400V) was applied between the mesh electrode that was 5 mm above the liquid surface and a Pt cell with 25 mm in diameter. Benzene solutions of porphyrin derivatives (tetraphynylporphyrin (TPP), Zn complex of TPP (Zn-TPP)) were prepared at the concentration of $1*10^{-4}$ M. The solution was added by 100 μL dropwisely on the surface of 5 mL water. After evaporating benzene for 5 min, the photoinduced current (~ 0.1 pA) was measured by a picoammeter (Keithley model 428).

Measured photoionization spectra were analyzed and threshold values were determined by fitting the spectra to the empirical formula of $I = (E - E_{th})^{2.5}$. Figure 1 shows the obtained photoionization current of Zn-TPP. The curve fits well and the threshold value was determined to 5.50 ±0.01 eV from repeated experiments (n = 5). The threshold values are listed in Table 1 as well as the reported values in vacuum [2].

All measured threshold lies higher in a vacuum because each molecule (E_{th}) satisfy the formula in the case of emitting electron into the air, $E_{th} = I_p + P^+$ where I_p and P^+ are the ionization potential and polarization energy of the photoionized molecule, respectively. P^+ is always negative since the polarization is exothermic. In the porphyrin case, the observed value P^+ is smaller than that for aromatic hydrocarbon (perylene, Table 1) because polarization energy reciprocally depends on the size of molecule and the size of porphyrin is approximately 2.1 times larger than perylene. However, this value is not enough for explaining the small polarization energy (1/2.5-3.0) compared to perylene. Further researches are now in progress for analyzing the result.

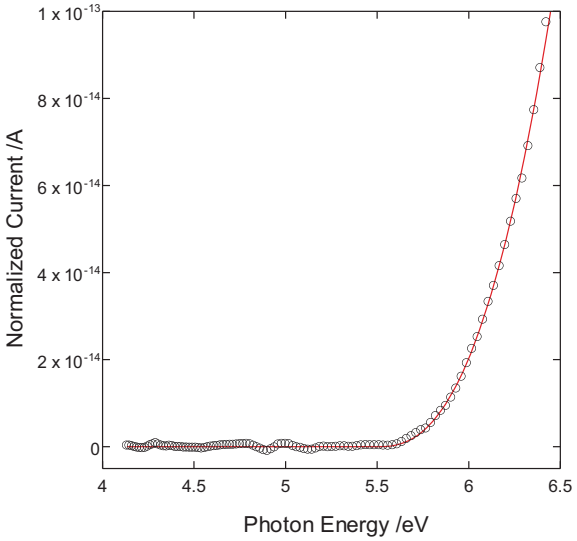

Fig. 1. Measured photoinduced current of Zinc Tetraphenylporphyrin at the surface of water. Inserted curve is the nonlinear fit using the formula $I = I_0 (E - E_{th})^{2.5}$.

Table 1. Photoionization threshold (E_{th}) of porphyrin derivatives at the water surface and their ionization potential (IP) in vacuum.

	E_{th} / eV	IP / eV
TPP	5.65 ± 0.04	6.3 ± 0.2*
Zn-TPP	5.50 ± 0.01	6.0 ± 0.2*
Pyrene	5.30 ± 0.04**	6.960

*) Ref.[2] **)Ref.[3]

[1] N. Inoue, T. Ishioka and A. Harata, Chem. Lett. **38** (2009) 358.

[2] Y. Nakano *et al.*, Chem. Phys. Lett. **39** (1976) 358.

[3] T. Ishioka, K. Tomita, Y. Imanishi and A. Harata, UVSOR Activity Report **39** (2012) 63.

BL4B

Multi-Electron Spectroscopy for Condensed H_2O Molecules

Y. Konosu, M. Sawa, K. Soejima and Y. Hikosaka
Niigata University, Niigata 950-2181, Japan

Slow electron formation has received particular attention, in connection with DNA strand breaks in living cells exposed to ionizing radiations. The DNA strand breaks are caused, not only by direct ionization of the DNA itself, but also by the impact of secondary particles produced by the radiation. Here, the most abundant secondary particles are electrons emitted from the ionization of water molecules and biomolecules surrounding the DNA, where the majority of the electrons have kinetic energies of less than 20 eV. The efficiency of the DNA strand breaks is strongly dependent on the incident electron energy of the impacting electrons, due to its resonant character, and therefore the knowledge of the energy distribution of the slow electrons is important in modeling the radiation damages of living cells. In this study, we have investigated the slow electron emission process of condensed H_2O irradiated with soft x-ray.

The experiments were carried out by using a magnetic bottle-type electron energy analyzer. A copper wire of a 0.3-mm diameter was placed at the focus point of the monochromatized synchrotron radiation, and was cooled with liquid nitrogen, in order to condense H_2O vapor admitted into the chamber. Figure 1 shows total electron yield spectra around the O1s range, measured before and after the cooling of the copper wire. The spectrum measured before the cooling shows structures attributable to electrons from CuO formed on the copper wire surface. After cooling, the spectral feature changes drastically, implying that H_2O molecules are adsorbed on the surface.

The energy correlation between two electrons emitted from condensed H_2O is shown in Fig. 2. On the map clear structures due to coincidences between photoelectrons and Auger electrons are seen, which proves that the magnetic bottle-type electron energy analyzer enables us to investigate the energy correlations among electrons emitted from condensed H_2O. Figure 3 shows the energy correlation between photoelectrons and slow-electron observed in triple coincidence events including Auger electrons. The right panel represents the slow electron spectrum extracted by integrating the coincidence yields in the horizontal range for the O1s photoelectrons. It is estimated, from the total coincidence counts in this curve and the photoelectron yields, that the decay path emitting the slow electrons is about 0.18% of the $O1s^{-1}$ creation. This ratio for gas-phase H_2O is reported to about 13% [1], and the emission of slow electron is reduced in the condensation. The reasons of the less efficient sole electron formation from the condensed H_2O are as follows. In the case of gas-phase H_2O, the main source of slow electron is autoionizing O^* fragment formed by double OH-bond breaking at highly-excited H_2O^{2+} states populated after Auger decay of the O1s core-hole state. This dissociation at the H_2O^{2+} states should be largely inhibited in the condensed phase by the neighboring H_2O molecules. Moreover, while such dissociations could occur and emit slow electrons, a considerable part of the slow electrons would fail to escape from the condensed H_2O molecules.

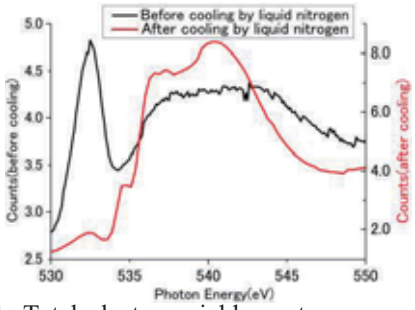

Fig. 1. Total electron yield spectra measured before and after the cooling of the copper wire.

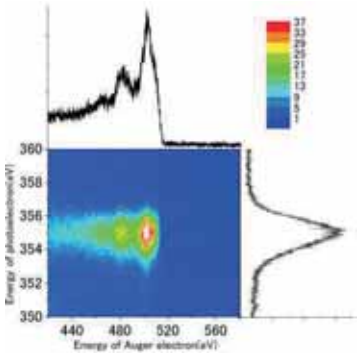

Fig. 2. Energy correlation between photoelectrons and Auger electron emitted from condensed H_2O. The photon energy was set to 900.1 eV.

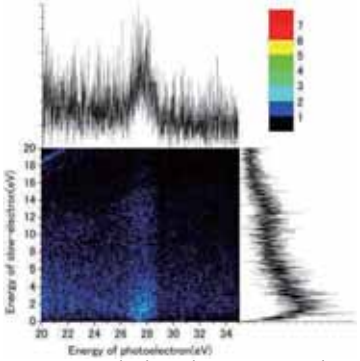

Fig. 3. Energy correlation between photoelectrons and slow-electron.

[1] Y. Hikosak *et al*., J. Chem. Phys. **137** (2012) 191101.

BL4B

Molecular Orientation and Magnetic Property of Vanadium Phthalocyanine Multilayer on a Silver Surface Studied by XAS/XMCD

K. Eguchi[1], Y. Takagi[1, 2], T. Nakagawa[1, 2] and T. Yokoyama[1, 2]

[1] *School of Physical Sciences, The Graduate University for Advanced Studies (SOKENDAI), Okazaki 444-8585, Japan*

[2] *Division of electronic structure, Institute for Molecular Science, Okazaki 444-8585, Japan*

3d transition metal phthalocyanines (TMPcs) have attracted much interest in recent years because they show characteristic electronic, optical and magnetic properties. In our group, we have especially focused on the magnetic properties of TMPcs to understand their magnetic coupling in their films and between TMPcs and ferromagnetic surfaces [1-3]. For instance, iron phthalocyanine (FePc) in multilayer shows a ferromagnetic behavior [2]. Recently, we have succeeded in preparing a vanadium phthalocyanine (VPc) multilayer. In this study, we have investigated the molecular orientation and magnetic property of the VPc multilayer by means of x-ray absorption spectroscopy (XAS) and x-ray magnetic circular dichroism (XMCD).

The experiments were carried out in an ultra high vacuum condition at beam line 4B. A silver film was prepared on a clean Cu(111) substrate by the electron bombardment evaporation at room temperature (RT). Purified H_2Pc and Vanadium atoms were deposited on the substrate at RT using Knudsen cell and electron beam evaporation source, respectively. The N *K*-edge and V *L*-edge XAS/XMCD measurements were done using a system (JANIS: 7THM-ST-UHV) with a superconducting magnet and a liq. He cryostat. The XAS and XMCD spectra were taken at 5 K and the XMCD spectra were recorded with reversal magnetic field.

Figure 1 shows angle dependence of N K-edge XAS spectra of 10ML VPc. The π* resonance intensity is observed at normal incidence and the intensities increase with increasing the incident angle. This result means that the framework of the phthalocyanines is slantingly tilted from the substrate surface plane.

Figure 2 shows V $L_{2,3}$-edge XMCD spectra of 10ML-VPc and VOPc [4] taken at an external magnetic field of 5 T and an incident angle of 55 degree. The spectra of VPc are obviously different from ones of VOPc at both V *L*-edge and O *K*-edge. The XMCD signal of VOPc is observed because it has one electron in 3d-orbital. On the other hand, that of VPc is very small in comparison to that of VOPc even though a vanadium atom in VPc has 3 electrons in 3d-orbital. This result might indicate that vanadium atoms in VPc are antiferromagnetically coupled. To reveal it, we need to investigate for the case of 1ML-VPc which has no magnetic interaction between them.

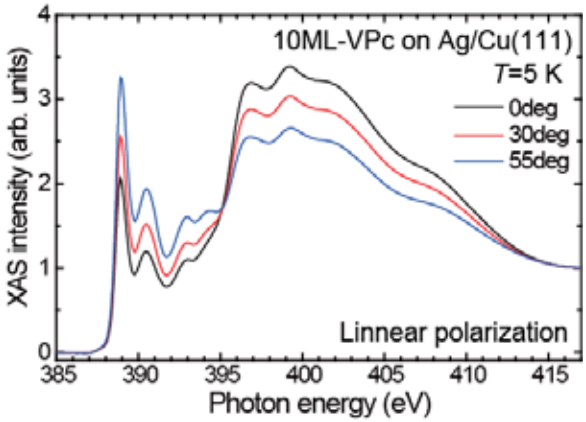

Fig. 1. The angle dependent N *K*-edge XAS spectra of VPc multilayer.

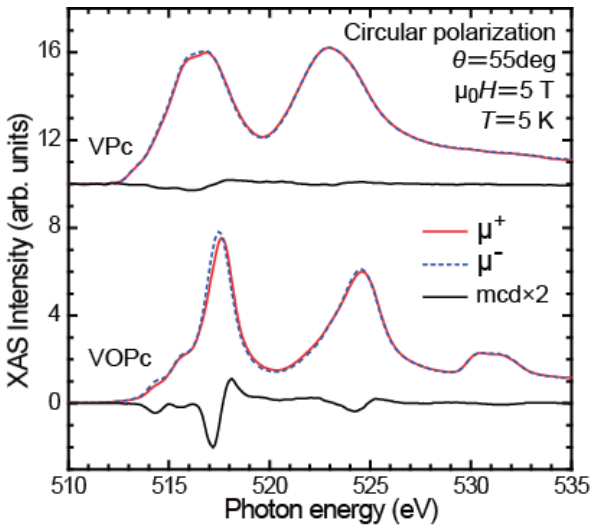

Fig. 2. V $L_{2,3}$- (and O *K*) edges XAS and XMCD spectra of VPc and VOPc multilayers taken at the incident angle of 55 deg, $\mu_0 H$=5 T and *T*=5 K.

[1] I. Yamamoto, K. Eguchi, Y. Takagi, T. Nakagawa and T. Yokoyama, UVSOR Activity Report **37** (2010) 74.

[2] Y. Takagi, K. Eguchi, T. Nakagawa and T. Yokoyama, UVSOR Activity Report **38** (2011) 67.

[3] Y. Takagi, K. Eguchi, T. Nakagawa and T. Yokoyama, UVSOR Activity Report **39** (2012) 66.

[4] K. Eguchi, Y. Takagi, T. Nakagawa and T. Yokoyama, UVSOR Activity Report **39** (2012) 65.

XMCD Studies of Magnetization of Co Ultrathin Films on W(110)

T. Nakagawa[1, 2, 3], H. Nakano[2, 4], K. Eguchi[2, 3], Y. Takagi[2, 3] and T. Yokoyama[2, 3]
[1]*Department of Molecule and Material Sciences, Kyushu University, Kasuga 816-8580, Japan*
[2]*Institute for Molecular Science, Okazaki 444-8585, Japan*
[3]*The Graduate University for Advanced Studies (SOKENDAI), Okazaki 444-8585, Japan*
[4]*Department of Chemistry, Graduate School of Science, Kyoto University, Kyoto 606-8502, Japan*

Magnetic properties in ultra thin films have attracted interests because of their characteristics due to low dimensionality [1-3]. Co ultrathin films, including nano wire and nano dots, have been extensively studied since they exhibit large magnetic anisotropy [1, 2]. Co films grown on W surfaces have been investigated since it shows sharp interface without no alloying. One of the long standing issues on Co/W(110) is vanishing magnetization below 2 monolayer (ML).

We performed experiments at BL4B using x-ray magnetic circular dichroism (XMCD) end station equipped with a superconducting magnet under $H = 5$ T and $T_s = 5$ K. All the measurements were done below 1×10^{-10} Torr. The Co films were grown on W(110) at room temperature, which was cleaned by repeated cycles of oxidation at 1500 K and subsequent annealing at 2200 K. The Co film shows psedomorphic structure bwlow 0.6 ML, and above this coverage it shows close packed structures. All the XMCD results are taken on the close packed structures.

Figure 1(a) shows x-ray absorption spectra (XAS) using circularly polarized light with opposite magnetization directions and XMCD spectrum for 0.9 ML. The 0.9 ML Co film shows no detective XMCD signal even in the low temperature (5 K) and high magnetic field (5 T). This result ensures that the Co film is not in a ferromagnetic order or has extremely high magnetic anisotropy, but the latter case is unlikely since the magnetic anisotropy greater than 50 T is necessary to explain the negligible XMCD signal. This vanishing XMCD result is in good agreement with previous studies [1, 2].

Figure 1(b) shows a magnetization curve taken on 1.7 ML Co film. The 1.7 ML Co film exhibits perpendicular magnetic anisotropy with a coercive field of 1.7 T, which is large compared to that of the bulk Co (~0.1 T). Thus the magnetization easy axis for 1.7 ML Co film is perpendicular to the surface, which is revealed for the first time. In the previous measurements the Co film did not show ferromagnetic states between 1 and 2 ML. The failure to detect the perpendicular magnetization may come from its large coercivity.

Figure 1(c) shows a magnetization curve for 4 ML Co film. This shows in-plane magnetization with 1.5 μ_B, which is in agreement with the previous results [1, 2].

These result demonstrates that the Co film grown on W(110) surface undergoes a spin reorientation transition from the perpendicular to the in-plane axis with increasing the Co coverage. Below 1 ML the total magnetization is almost zero. The XMCD measurement rules out the existence of huge anisotropy. The vanishing magnetization would be caused by quenching of Co magnetic moment due to a strong hybridization between Co and W or anti-ferromagnetism (or spin density waves).

[1] G. Garreau, M. Farle, E. Beaurepaire and K. Baberschke, Phys. Rev. B **55** (1997) 330.
[2] A. Kleibert, V. Senz, J. Bansmann and P. M. Oppeneer, Phys. Rev. B **72** (2005) 144404.
[3] T. Nakagawa, Y. Takagi, T. Yokoyama, T. Methfessel, S. Diehl and H.J. Elmers, Phys. Rev. B **101** (2012) 144418.

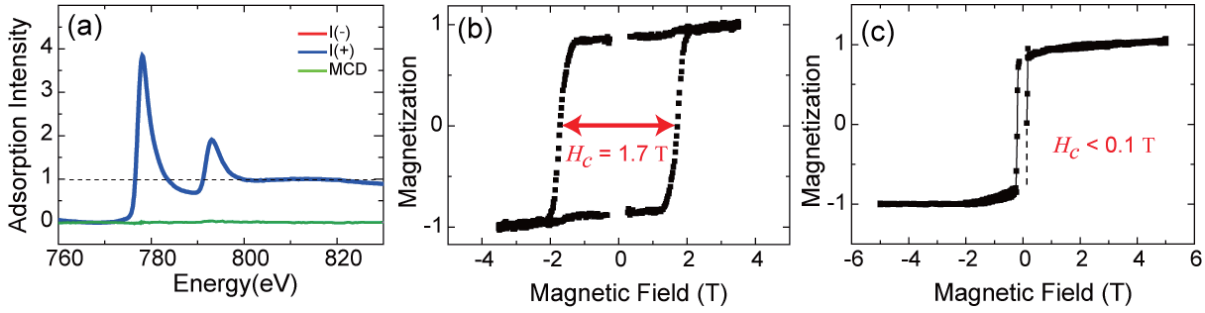

Fig. 1. XMCD results on Co/W(110) surfaces. (a) x-ray adsorption and XMCD result on Co(0.9 ML)/W(110) surface, showing no dichroic signal. (b) A magnetization curve obtained from XMCD measurement on Co(1.7 ML)/W(110) surface. Magnetic field is applied normal to the surface. (c) A magnetization curve obtained from XMCD measurement on Co(4.0 ML)/W(110) surface. Magnetic field is applied along the direction which is tilted 30° to the [1-10] direction.

BL4B

X-ray Magnetic Circular Dichroism Studies of Monolayer Iron Phthalocyanine Molecules Grown on Single and Bilayer Graphene

M. Ohtomo[1], Y. Matsumoto[1], S. Entani[1], P. V. Avramov[1], H. Naramoto[1], T. Yokoyama[2] and S. Sakai[1]

[1] *Advanced Science Research Center, Japan Atomic Energy Agency, Tokai-mura, Ibaraki 319-1195, Japan*

[2] *Department of Materials Molecular Science, Institute for Molecular Science, Okazaki, Aichi 444-8585, Japan*

Graphene is a promising spintronics material for its long spin diffusion length as a consequence of small spin-orbit coupling [1]. There are also numbers of reports on the functionalization of graphene using finite geometries, adatoms or defects [2]. The adsorption of magnetic adatoms or molecules, for example, open the possibility for controlling the intrinsic spintronic properties of graphene through so -called Ruderman-Kittel-Kasuya-Yoshida ı (RKKY) coupling between magnetic molecules or defects.

Previous theoretical works on the RKKY coupling in graphene [3-5] have shown that for all bipartite lattices at halffilling, the RKKY coupling is ferromagnetic (FM) for impurities on the same sub-lattice but antiferromagnetic (AFM) for impurities on different sub-lattices. However, there are no reports of the experimental observation of RKKY interaction in graphene. In our beam time, we performed series of X-ray magnetic circular dichroism (XMCD) measurements on ultra-thin magnetic molecules/graphene hetero structure.

The monolayer film of Iron phthalocyanine (FePc) was grown on three graphene samples: bilayer graphene (BLG) on Cu(111), single layer graphene (SLG) on SiC(0001) and highly ordered pyrolytic graphite (HOPG) as a reference. The samples were thoroughly degassed in ultra-high vacuum chamber at 500˚C before the deposition of FePc.

Fig. 1 shows Fe $L_{2,3}$-edge XMCD of monolayer FePc/SLG hetero structure at magic angle (55˚) incidence (MI). The spectrum shape of $L_{2,3}$ edge adsorption was identical with that of FePc textured thin film [6], which suggest ^3E_g ground state meaning small interaction with the substrate. Similar X-ray adsorption spectra were observed for FePc/BLG and FePc/HOPG as well. Due to large orbital moment of FePc molecules, smaller XMCD signal was observed in case of normal incidence (NI) condition. The magnetic field dependence of the XMCD signals is shown in Fig. 2 for FePc/BLG sample, which did not show saturation behavior up to 5 T.

In order to confirm the possibility of super paramagnetic component, we assumed the blocking temperature around 50 K and measured XMCD at "field cool" and "zero-field cool" conditions, which showed no differences within experimental error (not shown). This result indicates two possibilities, that is, the blocking temperature was larger than 50 K, or magnetic coupling was negligibly small. It was recently reported that the conduction electrons in graphene interact with magnetic defects (carbon atomic vacancies) thorough Kondo effect [7]. This report together with our XMCD results suggest that the transport property of FePc/graphene nano composite should be investigated as well in order to understand the nature of electron-electron interaction in the system.

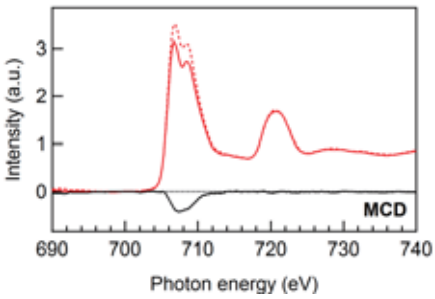

Fig. 1. Fe $L_{2,3}$-edge XMCD spectra of monolayer FePc/SLG hetero structure. The temperature was 5.4 K with applied magnetic field of ±50 kOe.

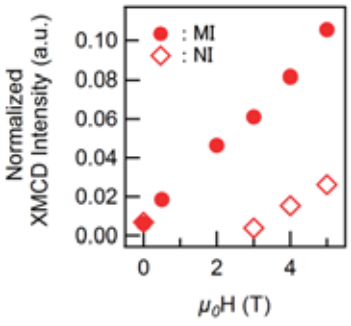

Fig. 2. The magnetic field dependence of XMCD signals in case of FePc/BLG nano-composite. The temperature was 5.5 K during the measurement.

[1] B. Dlubak *et al*., Nature Phys. **8** (2012) 557.
[2] O. V. Yazyev, Reports on Progress in Physics **73** (2010) 056501.
[3] A. M. Black-Schaffer, Phys. Rev. B **81** (2010) 205416.
[4] E. Kogan, Phys. Rev. B **84** (2011) 115119.
[5] M. Sherafati *et al*., Phys. Rev. B **84** (2011) 125416.
[6] J. Bartolomé *et al*., Phys. Rev. B **81** (2010) 195405.
[7] J. H. Chen *et al*., Nature Phys. **7** (2011) 535.

Temperature Dependence of the Electronic Structure of K-doped EuO Ultrathin Film

H. Momiyama[1], H. Miyazaki[2], T. Hajiri[1,3], M. Matsunami[3,4], T. Ito[1] and S. Kimura[3,4]

[1]*Graduate School of Engineering, Nagoya University, Nagoya 464-8603, Japan*
[2]*Center for Fostering Young and Innovative Researchers, Nagoya Institute of Technology, Nagoya 466-8555, Japan*
[3]*UVSOR Facility, Institute for Molecular Science, Okazaki 444-8585, Japan*
[4]*School of Physical Sciences, The Graduate University for Advanced Studies (SOKENDAI), Okazaki 444-8585, Japan*

Europium monoxide (EuO), a ferromagnetic semiconductor, with Curie temperature (T_C) of 69 K, is attracting attention due to its anomalous magneto-optical and transport properties [1, 2]. Especially, T_C achieves to as high as 200 K in the electron doping case, recently. Therefore EuO is one of the candidate compounds for next-generation spintronics applications such as spinfilter. So far, we successfully fabricated single-crystalline EuO ultrathin films with a few atomic layers for device development by using molecular beam epitaxy (MBE) method. Furthermore, we have performed angle-resolved photoemission spectroscopy (ARPES) to clarify the electronic structure and its relation to the anomalous properties. Consequently, we revealed that the T_C decreases with reducing the thickness because of the weakening of hybridization strength of Eu 4*f* – O 2*p* and Eu 4*f* – Eu 5*d* [3].

In this study, we had fabricated K-doped EuO ultrathin film to elevate T_C. And we performed ARPES at the beamline BL5U of UVSOR- Ⅲ combined with the MBE system.

Figure 1 shows the temperature-dependent ARPES spectra of single-crystalline K-doped EuO ultrathin film (5nm) measured at hν = 38 eV, which corresponds to the trace around the X point. Eu 4f state has two structures at 1.4 eV (A) and 2.2 eV (B) binding energies. According to the previous research on EuO single-crystalline ultrathin film (5nm) [4], the former originates from the Eu 4*f* – O 2*p* and Eu 5*d* hybridized states being attributed to the magnetic property, while the latter from the bare Eu 4*f* states. In Fig. 1, we found that the feature A gradually shifts to the lower binding-energies below 100 K. The observed shift could be originated in the exchange energy splitting below T_C of around 100 K. In turn, it is suggestive of the elevated T_C on the K-doped EuO than EuO ultrathin film. To clarify the detailed effect of K-doping, further studies are intended.

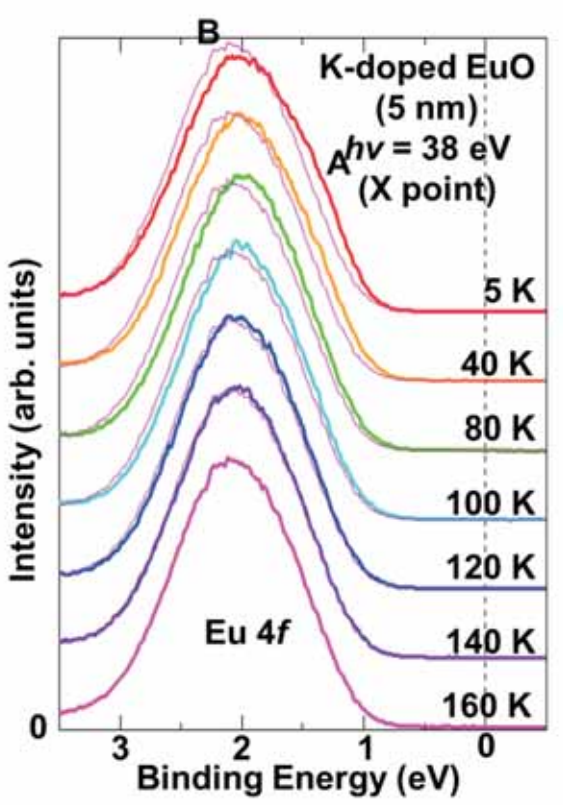

Fig. 1. Temperature dependent ARPES spectra of K-doped EuO ultrathin film (5nm) measured at hν = 38 eV. The thin lines are ARPES spectra in 160 K for comparison.

[1] N. Tsuda *et al*., *electronid Conduction in Oxides* (Springers College) (1976).
[2] A. Mauger *et. al.,* J. Phys. (paris) **39** (1978) 1125.
[3] H. Miyazaki *et al*., UVSOR Activity Report **39** (2012).
[4] H. Miyazaki *et al*., Phys. Rev. Lett. **101** (2009) 227203.

BL5U

Soft X-ray Photoelectron Spectroscopy Study of $Fe_2P(0001)$

K. Edamoto[1, 2] and Y. Sugizaki[1]

[1]*Department of Chemistry, Rikkyo University, Nishi-Ikebukuro, Toshima-ku, Tokyo 171-8501, Japan*

[2]*Research Center for Smart Molecules, Rikkyo University, Nishi-Ikebukuro, Toshima-ku, Tokyo 171-8501,Japan*

The surface properties of transition metal phosphides (TMPs) have attracted much attention because these materials have been shown to have high catalytic activities for HDS and HDN [1]. Of all TMPs studied thus far, Ni_2P has the highest catalytic activity, while that of Fe_2P has been found to be very low [1]. The high catalytic performance of Ni_2P has been proposed to arise from the stabilization of active Ni sites induced by segregation of substrate P atoms toward the surface [2]. In order to elucidate the origin of the high activity of Ni_2P, we think that it is useful to elucidate the difference in surface properties of Ni_2P and Fe_2P. However, in contrast to the accumulation of data on Ni_2P, very limited information is available as to the Fe_2P surfaces. In this work, we performed a soft X-ray photoelectron spectroscopy (SXPES) study on $Fe_2P(0001)$.

The experiments were performed at BL-5U of UVSOR, Institute for Molecular Science. The photoelectrons were collected by an electron energy analyzed of hemispherical type (MBS A-1), using an angle-integrated mode (acceptance angle of ±20°). The Fe_2P single-crystal was grown by Dr. S. Otani of National Institute for Materials Science. The sample was cut at an orientation of (0001) by spark erosion, and the surface was polished mechanically to a mirror finish. The surface was cleaned by several cycles of Ar^+ ion sputtering and annealing (600℃) in the UHV system.

Figure 1 shows SXPES spectra of $Fe_2P(0001)$ measured at various photon energies of 48 – 60 eV. A clear cut-off at the Fermi edge is observed independent of the photon energy, indicating a metallic nature of Fe_2P. A band is observed at 0 – 4 eV independent of $h\nu$. The band is ascribed to a Fe 3d – P 3p hybrid band (main band). Satellite peaks are observed at 5 and 7 eV, and these peaks are increased in intensity around the photon energy region of Fe 3p photoexcitation threshold ($h\nu$ = 54 eV). Therefore, the satellites are associated with the photoemission process including the Fe 3p – 3d photoexcitation and the following Fe 3d electron emission through a super-Coster-Kronig decay. At $h\nu$ > 56 eV, an additional band composed of photoelectrons with constant kinetic energy (44 – 45 eV) is observed, and the band is ascribed to a Fe MVV Auger peak.

The overall spectral features of $Fe_2P(0001)$ are similar to those of $Ni_2P(0001)$ [3]. In Fig. 2, the normal-emission spectrum of $Ni_2P(0001)$ is shown together with the spectrum of $Fe_2P(0001)$. Both spectra are measured at $h\nu$ = 48 eV. For $Ni_2P(0001)$, the main band is also observed at 0 – 4 eV. However, the main band is more stabilized and DOS around E_F is more suppressed for $Ni_2P(0001)$. It is considered that the stabilization of Ni 3d levels is essential to prevent the accumulation of S atoms on active metal sites in HDS for Ni_2P, which is less effective for Fe_2P.

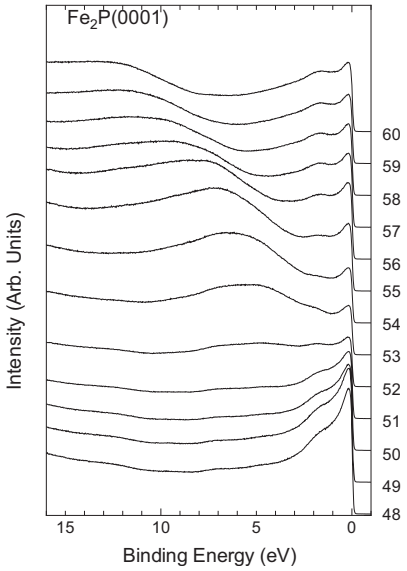

Fig. 1. Valence band spectra of $Fe_2P(0001)$.

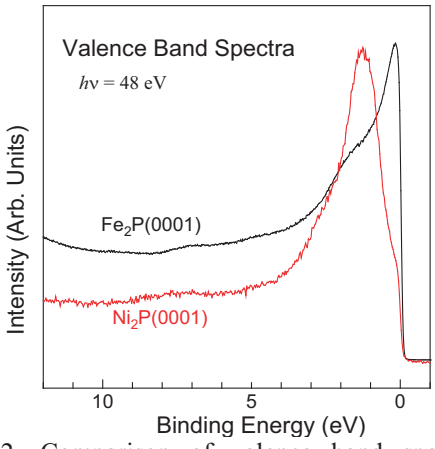

Fig. 2. Comparison of valence band spectra of $Fe_2P(0001)$ and $Ni_2P(0001)$.

[1] S. T. Oyama, J. Catal. **216** (2003) 343.
[2] K. Edamoto, Appl. Surf. Sci. **269** (2013) 7.
[3] K. Edamoto *et al.,* Solid State Commun. **148** (2008) 135.

BL5U

Characterization of Electronic Structures of Ge and $Ge_{1-x}Sn_x$ Surfaces by Using Angle-Resolved Photoelectron Spectroscopy

O. Nakatsuka[1], S. Ike[1], T. Asano[1], M. Kurosawa[1,2], N. Taoka[1], M. Matsunami[3], S. Kimura[3] and S. Zaima[1]

[1]*Graduate School of Engineering, Nagoya University, Furo-cho, Chikusa-ku, Nagoya 464-8603, Japan*
[2]*JSPS Research Fellow, 5-3-1 Kojimachi, Chiyoda-ku, Tokyo 102-0083, Japan*
[3]*UVSOR Facility, Institute for Molecular Science, Okazaki 444-8585, Japan*

Germanium (Ge), strained-Ge, and germanium-tin ($Ge_{1-x}Sn_x$) alloy are attractive candidates for high mobility channel material alternative to silicon (Si) in metal-oxide- semiconductor filed effect transistors (MOSFETs) in order to improve on ultra-large scale integrated circuits (ULSIs). $Ge_{1-x}Sn_x$ alloy with a Sn content high than 10% is also expected to be direct transition semiconductor. Theoretical calculation promises the reduction in the effective mass of holes in tensile strained Ge and compressive strained $Ge_{1-x}Sn_x$ compared to bulk-Ge and strained Si. Recently, we achieved the epitaxial growth of $Ge_{1-x}Sn_x$ thin films with wide Sn content (0~27%) on various substrates such as Ge, Si, and InP [1-3]. It is essentially important to understand the electronic properties of energy band dispersion, effective mass of electrons and holes, and carrier mobility of strained Ge and $Ge_{1-x}Sn_x$ alloy for ULSI applications. However, there are few reports about the electronic structure of strained Ge and $Ge_{1-x}Sn_x$.

In this study, we prepared the compressive-strained $Ge_{1-x}Sn_x$ epitaxial layers on Ge substrates, and investigated the electrical structures of Ge and $Ge_{1-x}Sn_x$ by using angle-resolved photoelectron spectroscopy (ARPES) measurement.

Ge(001) and Ge(110) wafers were used for substrates. After chemically cleaning, a Ge substrate was thermally cleaned in an ultra high vacuum chamber. Then, a 200 nm-thick $Ge_{1-x}Sn_x$ layer was deposited at 150~170°C on a Ge substrate. Sn content was ranging from 4.6% to 6.0%, which was estimated with x-ray diffraction two dimensional reciprocal space mapping. Successively, A 1~2 nm-thick Ge cap layer was deposited. Samples were brought to UVSOR/BL5U, and then introduced into a preparation UHV chamber connected to the ARPES measurement chamber. A sample was annealed at as high as 460°C in the preparation chamber in order to remove surface native oxide. Clean surface was confirmed from the surface reconstruction structure by using reflective high-energy electron diffraction (RHEED) observation. Samples were cooled at 15K during the ARPES measurement. ARPES measurement was performed with x-ray energies of 66 and 33 eV for $Ge_{1-x}Sn_x$/Ge(001) and $Ge_{1-x}Sn_x$/Ge(110) samples, respectively.

Figure 1 shows a typical ARPES result for the $Ge/Ge_{0.968}Sn_{0.032}$/n-Ge(001) sample. The spectra were measured for various take-off-angles (TOA). We can clearly see the energy dispersion related to the valence bands of light and heavy holes at the Γ-point. We have also obtained photoemission spectra from the strained-$Ge_{1-x}Sn_x$/Ge(110) and tensile-strained Ge/ $Ge_{1-x}Sn_x$/Ge(001) samples. The analysis of electronic structures and effective mass for holes are ongoing and will be reported in future.

We acknowledge members of Prof. Ujihara's group, Nagoya University for their kind support in the ARPES measurement.

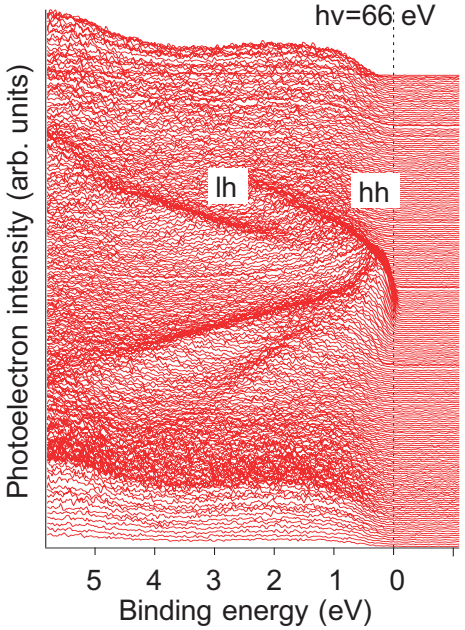

Fig. 1. Photoemission spectra with various TOAs (126 slices) for the $Ge/Ge_{0.968}Sn_{0.032}$/n-Ge(001) sample.

[1] S. Zaima, O. Nakatsuka, Y. Shimura, S. Takeuchi, B. Vincent, F. Gencarelli, T. Clarysse, J. Demeulemeester, K. Temst, A. Vantomme, M. Caymax and R. Loo, ECS Trans. **41** (2011) 231.
[2] S. Zaima, O. Nakatsuka, M. Nakamura, W. Takeuchi, Y. Shimura and N. Taoka, ECS Trans. **50** (2012) 897.
[3] O. Nakatsuka, Y. Shimura, W. Takeuchi, N. Taoka and S. Zaima, Solid-State Electron. **83** (2013) 82.

BL5B

Characterization of TiO_2/Sapphire Beam Splitter for High-Order Harmonics

H. Kumagai[1], M. Sanjo[1] and T. Shinagawa[2]

[1]*Graduate School of Engineering, Osaka City University, 3-3-138 Sugimoto, Sumiyoshi-ku, Osakashi, Osaka 558-8585, Japan*

[2]*Inorganic Materials Lab., Osaka Municipal Technical Research Institute, 1-6-50 Morinomiya,Joto-ku,Osaka 536-8553, Japan*

High-intensity high-order harmonic generation has been investigated intensively in recent years because of application to nonlinear optics with magnificent spatial coherence and with an ultrashort pulse duration for high peak power. In the development of beam line for high-intensity high-order harmonics, however, utilizing a conventional beam splitter (BS) (Si or SiC) that absorbs fundamental waves causes serious problems such as its thermal distortion [1]. To resolve these problems, we proposed and investigated novel BS with transparent materials that transmitted the fundamental waves and then reflected the high-order harmonics. In BS for the high-order harmonics, reflection of the fundamental waves should be prevented by entering the p-polarized fundamental waves at the Brewster's angle θ_B, which could improve the separation between the fundamental waves and the high-order harmonics.

Atomic layer deposition (ALD) and atomic layer epitaxy (ALE) are gas phase deposition methods that are based on sequential surface chemical reaction where the growth rate is dependent solely on the number of growth cycles. These deposition methods have emerged as the excellent techniques to fabricate a wide variety of thin films [2-6]. The main difference between ALE and chemical vapor deposition (CVD) is the way to introduce precursor into the reaction chamber. Unlike CVD, each precursor is alternately pulsed to the chamber in ALE process. ALE has self-limiting nature of the surface saturation, allowing the formation of a full or a sub-monolayer of atoms because adsorption of precursor gases stops due to covered surface reactive sites or steric hindrances of ligands of adsorbed molecules. It can coat complex shapes with excellent uniformity and control thickness with precision over large areas.

We have already studied and fabricated TiO_2 thin films on sapphire (0001) substrates by controlled growth with ALD or ALE. One of authors has already demonstrated that rutile TiO_2 (200) thin films were grown epitaxially on sapphire (0001) substrates by ALE using sequentially fast pressurized titanium tetrachloride ($TiCl_4$) and water (H_2O) vapor pulses [7].

Figure 1 shows reflectivity (p polarization) of TiO_2/sapphire BS. Incident angle θ_B was set at 70.5° for TiO_2 and at 65.56° for sapphire, which corresponded to the Brewster angles θ_B of the 800-nm pump pulse. Figure 1 indicated that the peak reflectivities of TiO_2/sapphire BS were high reflectivity of 44.8% (incident angle θ_B =70.5° for TiO_2) and 31.9% (incident angle θ_B =65.56° for sapphire) at 21.24 nm, which corresponded to the 37th order harmonics of the 800-nm pump pulse, respectively. Thus, the incident angle θ_B was set at 70.5° for TiO_2, which corresponded to the Brewster angle θ_B of the 800-nm pump pulse.

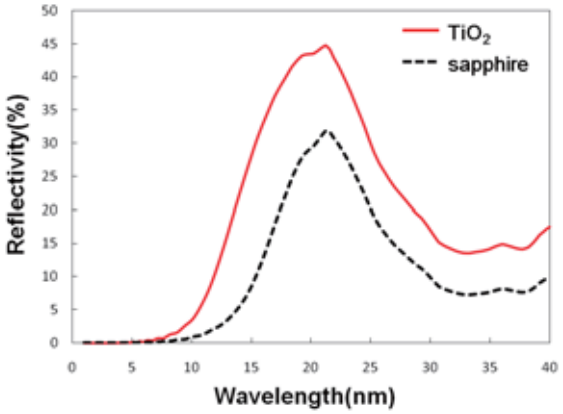

Fig. 1. Reflectivities of TiO_2/sapphire BS at the Brewster angles for TiO_2 (solid line) and sapphire (dashed line) at the pump pulse.

[1] E. J. Takahashi *et al.*, Opt. Lett. **29** (2004) 507.
[2] S. M. George *et al.*, J. Phys. Chem. **100** (1996) 13121.
[3] D. M. Hausmann *et al.*, Thin solid Films **443** (2003) 1.
[4] S. J. Kwon, Jpn. J. of Appl. Phys. **44** (2005) 1062.
[5] M. Ishii *et al.*, J. crystal Growth **180** (1997) 15.
[6] H. Kumagai *et al.*, J. Mater. Sci. Lett. **15** (1996) 1081.
[7] H. Kumagai *et al.*, J. Crystal Growth **314** (2011) 1.

BL6U

Spin-Orbit Coupled Gold Atomic Chains on Vicinal Si Surfaces

S. Won Jung[1], W. Jong Shin[1], H. Yamane[2], N. Kosugi[2] and H. W. Yeom[1]

[1] *Department of Physics and Center for Low Dimensional Electronic Symmetry, Pohang University of Science and Technology, Pohang 790-784, Korea*

[2] *Department of Photo-Molecular Science, Institute for Molecular Science, Okazaki 444-8585, Japan*

One dimensional (1D) electronic system has been studied for its exotic phenomena such as Peierls instability [1], and non-Fermi liquid behavior [2]. For the non-Fermi liquid, most experimental researches focused on the spin-charge separation [3] and the power-law dependent density of states near the Fermi level [4].

However, there has been almost no such study for the non-Fermi liquid state with the spin-orbit coupling [2-4]. Moreover, 1D systems with the spin-orbit coupling becomes important for spintronic applications and for finding Majorana Fermions [5, 6]. Therefore, 1D electronic system with a substantial spin-orbit coupling would be an important topic with a chance to observe exotic states such as Spiral Luttinger liquids and Helical Luttinger liqids [7].

In the present study, we performed angle-resolved photoelectron spectroscopy (ARPES) measurements, using BL6U of UVSOR, in order to measure the band structure of gold atomic wires formed on a vicinal silicon surface, Si(553). Gold atomic wires on vicinal Si surfaces has been known to possess multiple 1D metallic bands [8], Peierls instability [9], and Rashba-type spin-orbit coupling [10].

Fig. 1 shows low energy electron diffraction (LEED) images of two phases of Au atomic wires on Si(553) surface at different gold coverages. The periods along [1 1 -2] direction (perpendicular with wires) is $(4+1/3)a_0$ [Fig. 1 (a), A phase] , $(9+2/3)a_0$ [Fig. 1 (b), B phase]. The B phase is found for the first time in this work. However, in Fig. 2, the electronic structures have strong similarity with surface states, S1 and S2 (known as the Rashba spin splitting [10]) and S3. Therefore, we can assume that the two phases features the same gold chain structure with different density.

In this study, we measured high-resolution band spectra of the B phase, which is thought to have a lower wire density and thus a large interwire distance. We thus expect that this low density wire phase would exhibit a more ideal 1D electronic property and thus is a good candidate to investigate the possibility of non-Fermi liquid state with the spin-orbit interaction. The analysis of the spectra functions is underway along with a scanning tunneling microscopy study.

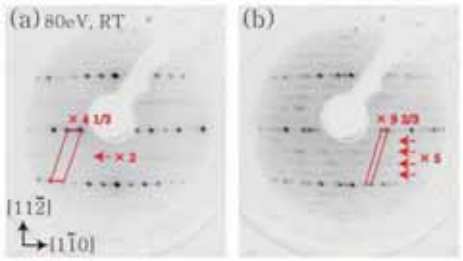

Fig. 1. Measured LEED images of Au atomic wires on Si(553). The coverage of Gold is about (a) 0.48ML, (b) 0.22ML. [1 -1 0] is the direction of atomic wires.

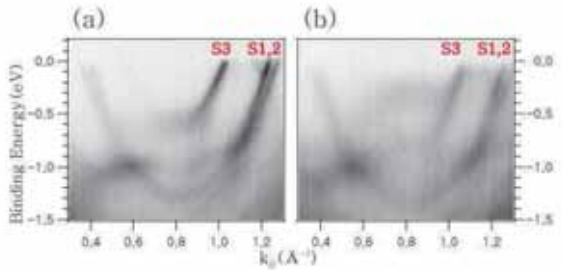

Fig. 2. Measured ARPES Spectra of Au atomic wires along [1 -1 0] direction with 46eV photon. The coverage of Gold is about (a) 0.48ML , (b) 0.22ML.

[1] H. W. Yeom *et al*., Phys. Rev. Lett. **82** (2009) 4898.

[2] T. Giamarchi, *Quantum Physics in One Dimension* (Clarendon Press, OXFORD, 2003).
J. N. Crain and F. J. Himpsel, Appl. Phys. A **82** (2006) 431.

[3] C. Kim *et al*., Phys. Rev. Lett. **77** (1996) 4054.

[4] Marc Bockrath *et al*., Nature **397** (1999) 598.
C. Blumenstein *et al*. ,Nature Physics **7** (2011) 776.

[5] R. M. Lutchyn, J. D. Sau, and S. Das Sarma, Phys. Rev. Lett. **105** (2010) 077011.

[6] J. Park *et al*., Phys. Rev. Lett. **110** (2013) 036801.

[7] B. Brauecker, C. Bena and P. Simon, Phys. Rev. B **85** (2012) 035136.

[8] J. N. Crain *et al*., Phys. Rev. Lett. **90** (2003) 176805.
J. N. Crain *et al*., Phys. Rev. B **69** (2004) 125401.

[9] J. R. Ahn, P. G. Kang, K. D. Ryang and H. W. Yeom, Phys. Rev. Lett. **95** (2005) 196402.

[10] I. Barke *et al*., Phys. Rev. Lett. **97** (2006) 226405.

Systematic Study on Intermolecular Interaction in Crystalline Films of Metal Phthalocyanine

H. Yamane and N. Kosugi
Department of Photo-Molecular Science, Institute for Molecular Science, Okazaki 444-8585, Japan

The intermolecular electronic band dispersion, originating from the periodicity of the molecular stacking structure, is essential to investigate the charge transport mechanism related to organic electronics. Recently, we have succeeded in observation of quite small intermolecular band dispersions for crystalline films of metal phthalocyanines (MPc, M = metal), such as ZnPc, MnPc, and F_{16}ZnPc, by the precise angle-resolved photoemission spectroscopy (ARPES) experiments [1]. These observations enable us to do systematic study of the intermolecular interaction in terms of the intermolecular distance along the π-π stacking direction ($a_\perp$) by changing terminal groups or central metals in the MPc molecule.

Figure 1(a) shows the normal-emission ARPES spectra as a function of the incident photon energy ($h\nu$) for a crystalline film of CoPc on Au(111) at 15K. The relative peak intensity between the highest occupied molecular orbital (HOMO) and HOMO-1 levels changes with $h\nu$. At $h\nu$ = 50 eV, the HOMO intensity is stronger than the HOMO-1 intensity. At $h\nu \geq 58$ eV, the HOMO-1 intensity is getting stronger than the HOMO intensity due to different ionization cross sections between the HOMO and HOMO-1 characters. This evidence indicates that the HOMO of CoPc is derived from the C 2p orbital; on the other hand, the HOMO-1 of CoPc is derived from the Co 3d orbital. These assignments agree well with theoretical results [2]. The HOMO (C 2p) and HOMO-1 (Co 3d) derived peaks show the clear periodic shift with $h\nu$. The periodicity of these dispersive peaks in the wave-vector space is explained by $a_\perp$ of 3.318 Å, which is evaluated from the X-ray diffraction (XRD) shown in Fig. 1(b). Therefore, it is concluded that the observed dispersive behavior for the HOMO and HOMO-1 peaks is ascribed to the delocalized band formation due to the intermolecular van der Waals interaction in the crystalline CoPc film.

From the observed band dispersions of the C-2p-derived band for crystalline films of various MPc molecules, the intermolecular transfer integral ($t_\perp$) can be evaluated with respect to $a_\perp$ as shown in Fig. 2. From the $t_\perp$-*vs.*-$a_\perp$ relation, we found that (i) the $t_\perp$ value is getting large with decreasing the $a_\perp$ value due to the stronger intermolecular electronic coupling and that (ii) the $t_\perp$-*vs.*-$a_\perp$ relation seems to be fitted by a linear function in the present narrow $a_\perp$ range. From the least-squares fitting, the slope parameter of $t_\perp/a_\perp$ is determined to be 70 meV/Å for the C-2p-derived band of α-crystalline MPc films.

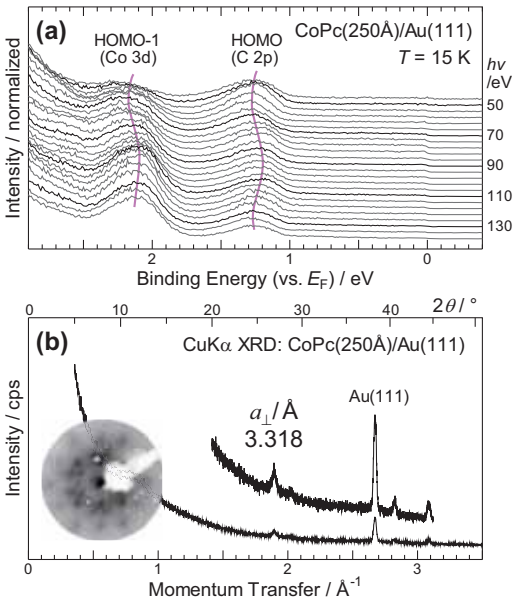

Fig. 1. (a) The photon energy ($h\nu$) dependence of the normal-emission ARPES spectra shown with the $h\nu$ step of 4 eV and (b) the CuKα X-ray diffraction (XRD) spectrum, measured for the crystalline CoPc film on Au(111). In panel (b), the low-energy electron diffraction image, taken at the incident electron energy of 34 eV, is also shown.

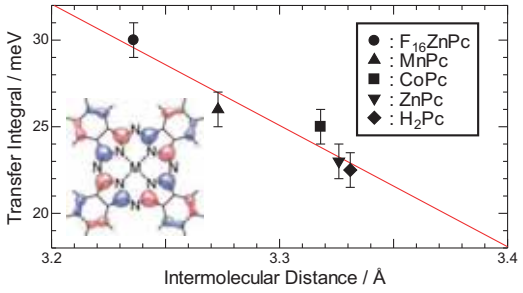

Fig. 2. The intermolecular transfer integral ($t_\perp$) with respect to the intermolecular distance along the π-π stacking direction ($a_\perp$) in flat-lying crystalline films of MPc on Au(111) at 15 K. The LCAO (linear combination of atomic orbitals) pattern of the C 2p derived level of MPc is shown in the inset.

[1] H. Yamane and N. Kosugi, submitted.
[2] For example, M.-S. Liao and S. Scheiner, J. Chem. Phys. **114** (2001) 9780.

BL6U

Crystallinity-Dependent Excited-Electron Dynamics in F_{16}ZnPc Films

H. Yamane and N. Kosugi

Department of Photo-Molecular Science, Institute for Molecular Science, Okazaki 444-8585, Japan

Resonant photoemission spectroscopy (RPES) has been applied to the study of the charge transfer dynamics at molecule/electrode interfaces [1, 2], which is called as a core-hole clock (CHC) experiment. The CHC method is based on the normal decay time of a core excitation (6 fs for N 1s) as a reference clock for other processes in the target system. That is, RPES signals depend on the timescale of excited electron motions with respect to that of the core-hole lifetime. Here we have applied the CHC method to the thick molecular films for the study of the excited-electron dynamics by the weak intermolecular interaction.

In the present work, we have used an archetypal n-type organic semiconductor of F_{16}ZnPc. In order to study the effect of the weak intermolecular interaction on the excited state, we have prepared an amorphous and a crystalline film of F_{16}ZnPc. The amorphous F_{16}ZnPc film is obtained by the molecular deposition onto a polycrystalline Au surface kept at the low temperature (T ~ 180 K). On the other hand, the crystalline F_{16}ZnPc film is obtained by the molecular deposition onto a single-crystalline Au(111) surface kept at the elevated temperature (T ~ 360 K). The sample crystallinity was confirmed by the N K-edge X-ray absorption spectroscopy (XAS), the low-energy electron diffraction, and the X-ray diffraction. For the crystalline F_{16}ZnPc film, furthermore, we confirmed that the valence band dispersion by the intermolecular interaction is observable. In order to avoid the effect of the molecular orientation on the core-level excitation, the N K-edge RPES and XAS spectra were measured at the magic-angle incidence geometry.

Figure 1 shows the color contour map of the N-K RPES spectra for (a) the amorphous and (b) crystalline F_{16}ZnPc film, measured at T = 15 K. We found that the ionization energy and the RPES intensity depend on the sample crystallinity. Among these, the RPES intensity, plotted in the upper panel of Fig. 1 together with the N-K XAS spectrum, is related to the excited-electron dynamics. The XAS spectra of both the amorphous and crystalline F_{16}ZnPc films show the first, second, and third N 1s $\rightarrow \pi^*$ transition peaks at the photon energy ($h\nu$) of 397.0, 399.4, and 401.4 eV, respectively. At these $h\nu$, the RPES spectra for the amorphous F_{16}ZnPc film also show the intensity maxima. On the other hand, for the crystalline F_{16}ZnPc film, the RPES intensity at $h\nu$ = 399.4 and 401.4 eV is decreased significantly. This evidence in RPES and XAS indicates that the timescale of the intermolecular charge transfer in the crystalline F_{16}ZnPc film is faster than that of the N 1s core-hole lifetime (6 fs) due to the delocalization of the excited electron. The intermolecular charge transfer time (τ_{CT}) can be determined from the modified equation given in Ref. [1] of

$$\tau_{CT} = \tau_{CH} (I_{cry\text{-}PE}/I_{cry\text{-}XA})(I_{amo\text{-}PE}/I_{amo\text{-}XA} - I_{cry\text{-}PE}/I_{cry\text{-}XA})^{-1},$$

where τ_{CH} is the core-hole lifetime, $I_{cry\text{-}PE}/I_{cry\text{-}XA}$ is the RPES/XAS intensity ratio for the crystalline film, and $I_{amo\text{-}PE}/I_{amo\text{-}XA}$ is the RPES/XAS intensity ratio for the amorphous film. Using this equation, the τ_{CT} in the crystalline F_{16}ZnPc film is determined to be 2.1 fs.

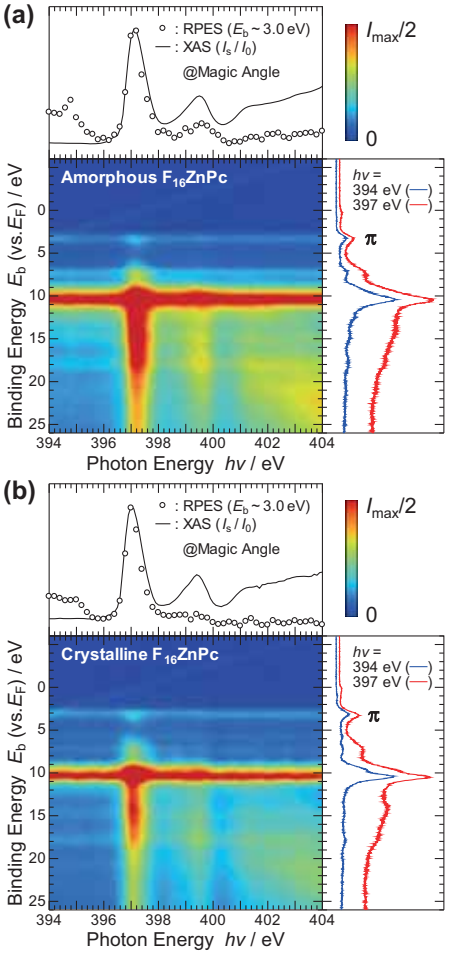

Fig. 1. Color contour map of the N-K RPES spectra for (a) amorphous and (b) crystalline films of F_{16}ZnPc at 15 K. Upper panel shows the intensity-vs-$h\nu$ profile at E_b = 3.0 eV (○), together with the XAS spectrum (–). Side panel shows the intensity-vs-E_b profile (*i.e.*, RPES spectrum) at $h\nu$ = 394 and 397 eV.

[1] P. A. Brühwiler, O. Karis and N. Mårtensson, Rev. Mod. Phys. **74** (2002) 703.
[2] L. Wang, W. Chen and A. T. S. Wee, Surf. Sci Rep. **63** (2008) 465, and references therein.

Anisotropy of Electron-phonon Coupling for Pentacene Monolayer

S. Kera[1], F. Bussolotti[1], H. Shinotsuka[1], N. Ueno[1], M. Matsunami[2] and S. Kimura[2]
[1]*Graduate School of Advanced Integration Science, Chiba University, Chiba 263-8522, Japan*
[2]*UVSOR, Institute for Molecular Science, Okazaki 444-8585, Japan*

Over the past decade, organic electronic devices have increased considerable attentions due to their potential applications. Fine features of the highest occupied molecular orbital (HOMO) state in highly-resolved ultraviolet photoelectron spectrum (UPS) of organic semiconductor can offer a variety of key information that is necessary to unravel fundamental mechanism in carrier-transport(transfer) properties in organic devices. Here, we present high-resolution angle-resolved UPS (ARUPS) studies on the HOMO hole in pentacene monolayer (ML) by using low-energy photon to access dynamic events of photohole.

ARUPS spectra were measured at photon incidence angle α=45°, hv = 7 to 10 eV and T=15 K at BL7U. The molecules were evaporated onto a clean graphite (HOPG) substrate. The coverage/thickness of the pentacene ML was confirmed by the binding energy (E_B) of HOMO[1,2]. No significant band dispersion is detected for the ML.

Figure 1 shows the angle-integrated UPS (for 36°) of pentacene ML. HOMO band is appeared at 1.3 eV. Vibronic satellites bands denoted by v = 1, 2, 3 and Lorentzian-like-tail feature are observed at higher-E_B and lower-E_B side, respectively [2]. We found the intensity ratio of hole-vibration coupling and the tail feature largely depends on the photoelectron kinetic energy.

To reveal the differences more precisely, photon energy dependences of ARUPS were recorded as shown in Fig.2. We found clear differences in the ARUPS intensity maps by using different photon energy of 0.8eV. The vibrational progression should follow a Poisson distribution under Frank-Condon approximation. The intensity of hole-vibration coupling, however depends largely on the momentum number, hence the momentum distribution curve (MDC) of vibronic peak is different from that of the main peak. It demonstrates that we have to consider a violation of Born-Oppenheimer approximation and dynamic photoemission processes for large-π conjugated materials.

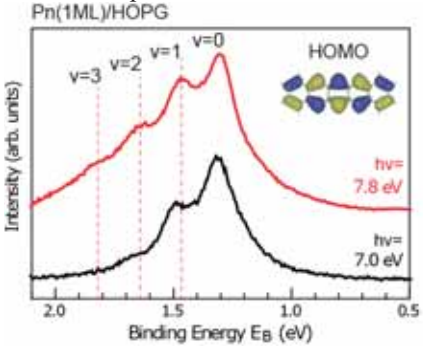

Fig. 1. Photon energy dependence of angle-integrated UPS of pentacene ML film prepared on a clean graphite (HOPG) (background subtracted).

Moreover, the low-E_B tail feature appears at around Γ point, which was accessible by observing low-kinetic-energy photoelectrons. The results may give a chance to discuss the origin of the HOMO band shape of molecular solids, which would be closely related to following topics: (i) accurate contribution of electron-phonon (hole-vibration) coupling to the hopping conduction. (ii) dynamics of polarization (molecular polaron and Holstein polaron) which is affected by lifetime of the photohole to give ~~a~~ the high-kinetic-energy tail of HOMO shape. To elucidate the anomalous features and their anisotropy, further studies are intended.

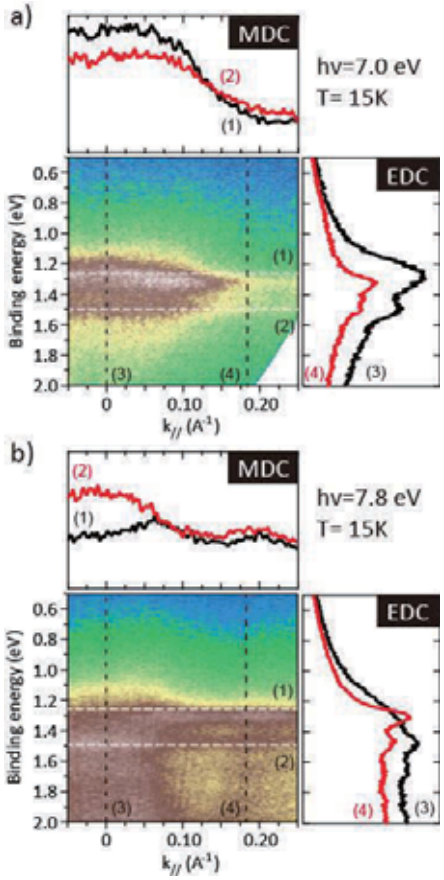

Fig. 2. ARUPS intensity map for pentacene ML/HOPG measured at hv=7.0eV a) and hv=7.8eV b). EDCs at $k_{//}$ = 0 and 0.18 (Δk= 0.04Å^{-1}) are shown in right panels. MDCs at E_B= 1.25 and 1.50 eV for ΔE= 0.05eV are shown in top panels.

[1] H. Yamane *et al.,* Phys. Rev. B **72** (2005) 153412.
[2] S. Kera *et al.*, Prog. Surf. Sci. **84** (2009) 135.

BL7U

Low-Energy Angle-Resolved Photoemission Study on Ultrathin Bi Films

T. Hirahara[1], M. Matsunami[2], T. Hajiri[2], S. Kimura[2] and S. Hasegawa[1]
[1]*Department of Physics, University of Tokyo, Tokyo 113-0033, Japan*
[2]*UVSOR Facility, Institute for Molecular Science, Okazaki 444-8585, Japan*

Semimetal bismuth (Bi) is one of the most extensively studied elements in solid state physics because of its extreme physical properties, such as the highest resistivity and Hall coefficient of all metals. Bi has tiny hole and electron pockets at *T* and *L* points, respectively, [Fig.1(a) and 1(b)], and therefore the Fermi wavelength λ_F is very large (about 30 nm). Because of this large λ_F, nanosized objects of Bi in the range of several tens of nanometers have been examined extensively toward the development of quantum-size-effect-based devices [1–3]. For example, the oscillation of the film resistance with the film thickness *d* was reported [4] and, furthermore, it was predicted that when the lowest quantized subband of the electron pocket is raised to an energy higher than the highest hole subband, a band gap will develop [semimetal-to-semiconductor (SMSC) transition at *d*~30 nm, Fig. 1(c)] [1, 5]. However, although many angle-resolved photoemission (ARPES) measurements have been performed on ultrathin Bi films, none has actually been able to verify whether this SMSC transition occurs or not [6-14]. The main reason is that the cross section for the bulk bands depends dramatically on the photon energy and polarization.

Therefore in the present study, we have performed ARPES measurements on ultrathin Bi films by systematically changing the photon energy (7-40 eV) and polarization (*P*- and *S*- polarization). Figures 2(a) and (b) show the band dispersion near the Fermi level at the Γ point (hν =9 eV). Whereas the well-studied surface states are observed clearly for the *P*-polarization data (a), they completely disappear in the *S*-polarization data (b). The hole-like dispersion in (b) suggests the detection of the bulk hole band and its maximum seems to be located below the Fermi level. This may be suggesting the occurrence of a SMSC transition. Further sophisticated study is needed to reach a definite conclusion.

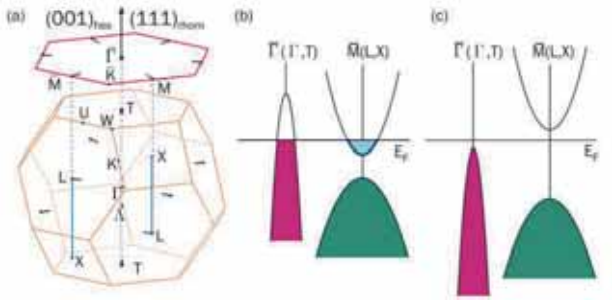

Fig. 1. (a) The Fermi surface of bulk Bi depicted in bulk (orange) and its projection to the surface (red) Brillouin zone. Electron (hole) pockets are filled with light blue (purple). (b), (c) Schematic drawing of the Bi bulk band projection near the Fermi level before (b) and after (c) the SMSC transition as predicted in Ref. [5].

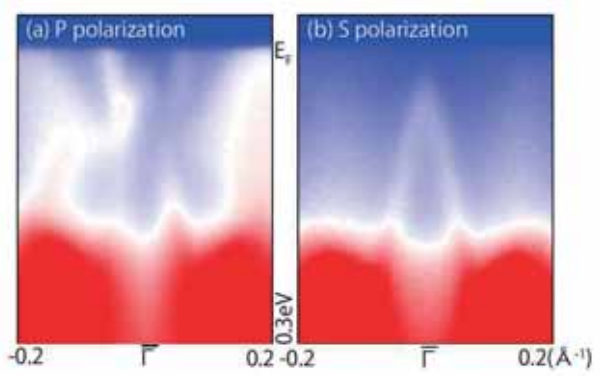

Fig. 2. The ARPES image of the band dispersion of Bi(111) films measured at hν=9eV for *P*- (a) and *S*- (b) polarized photons.

[1] C. A. Hoffman *et al.,* Phys. Rev. B **48** (1993) 11431.
[2] Z. Zhang *et al.,* Phys. Rev. B **61**, 4850 (2000).
[3] T. E. Huber *et al.,* Appl. Phys. Lett. **84** (2004) 1326.
[4] Yu. F. Ogrin *et al.,* JETP Lett. **3** (1966) 71.
[5] V. B. Sandomirskii, Sov. Phys. JETP **25** (1967) 101.
[6] T. Hirahara *et al.,* Phys Rev. Lett. **97** (2006) 146803.
[7] T. Hirahara *et al.,* Phys. Rev. B **75** (2007) 035422.
[8] T. Hirahara *et al.,* Phys. Rev. B **76** (2007) 153305.
[9] T. Hirahara *et al.,* New Jour. Phys. **10** (2008) 083038.
[10] A. Takayama *et al.,* Phys. Rev. Lett. **106** (2011) 166401.
[11] A. Takayama *et al.,* Nano Lett. **12** (2012) 1766.
[12] H. Miyahara *et al.,* eJSSNT **10** (2012)153.
[13] T. Okuda *et al.,* Rev. Sci. Inst. **82** (2011) 103302.
[14] G. Bian *et al.,* Phys Rev. B **80** (2009) 245407.

BL7U

Secondary Electron Emission from the Graphite Surface

S. Tanaka[1], M. Matsunami[2,3] and S. Kimura[2,3]

[1]*The institute of Scientific and Industrial Research, Osaka University, Ibaraki 567-0047, Osaka, Japan*

[2] *UVSOR Facility, Institute for Molecular Science, Okazaki 444-8585, Japan*

[3]*School of Physical Sciences, The Graduate University for Advanced Studies (SOKENDAI), Okazaki 444-8585, Japan*

When the condensed matter is electronically excited, the following relaxation process leads to the emission of many particles/waves such as phonons, photons, and electrons. For example, Graphite, one of the 'textbook' materials, emits 3.3-eV electrons when excited no matter what photon energy is used as shown in the right panel of Fig. 1, where other peaks change their kinetic energies as a function of the photon energy. This phenomenon is important not only from the scientific point of view, because it reveals the relaxation dynamics in solids, but also from the technical one, because it may leads to the development of the monochromatic electron emitter.

Previously, this 3.3eV peak has been ascribed to the electron emission from the unoccupied band located at 3.3eV above the vacuum level of the Graphite [1]. The photoexcitation process provides the electrons located at the unoccupied band, and they may be emitted with conserving their energies and momentum if its wavefunction is connected to the free-electron-like wavefunction in the vacuum. In this study, we chalenge this interpretation with using the two-dimensional photoelectron spectroscopy where both of the photon and kinetic energies are scanned.

The experiments were carried out at BL7U of UVSOR-III. The HOPG (highly oriented pyrolytic graphite) was cleaved *in-situ* and the surface-normal photoelectron spectra were recorded with the photon energy is scanned by 0.3-eV step for hν=6-16eV and 1-eV step for hν=16-26eV. The sample temperature was 13K for hν=6-16eV and 50K for hν=16-26eV. Significant differences were not observed when temperature was changed except anomalous peaks just below the Fermi level at lower temperature [2]. The photon intensity was calibrated by using the photo-diode.

The results for the surface-normal photoelectron emission, which correspond to the electron at the Γ-point in the Brillouin zone, are shown in center panel of Figure 1 as a colored map (red is higher than blue) where the x-axis indicates the photon energy and the y-axis indicates the kinetic energy of the photoelectron. The photoelectron intensities as a function of the electron-kinetic energy are plotted at the right panel at some photon energies and those as a function of the photon energy at some photon energies are shown in the upper panel. Dotted diagonal lines in the center panel shows the position of the peaks corresponding the photoexcitation from

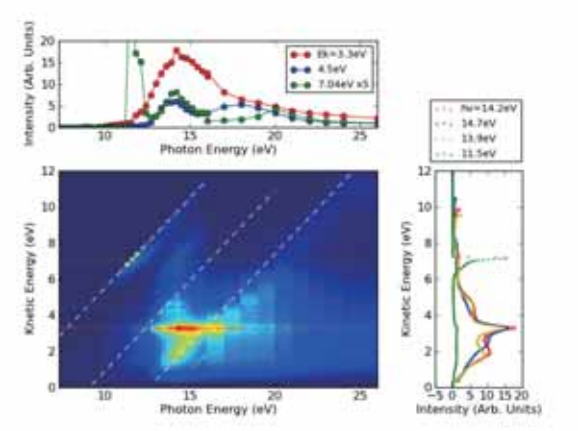

Fig. 1. Two-dimensional photoelectron spectra for HOPG Graphite.

the π-band (backfolded from the K-point [2]), the σ-band and the π-band, respectively, from the top to the bottom. The σ-band is hardly seen because it is prohibited by the dipole selection rule. Meanwhile, the horizontal lines correspond to the photoexcitation into a specific unoccupied state. Dotted lines are kinetic energies where high intensities are observed for several photon energies. The one who has the highest intensity is the 3.3-eV peak. According to the Fermi's golden rule, the photoexcitation probability resonantly increased when the photon energy agrees with the difference in energy between the occupied and unoccupied bands. These should be observed at the intersection points among the diagonal and horizontal lines. In the case of 3.3-eV peak, however, there is no particular enhancement at those photon energies. It clearly excludes the interpretation that the 3.3-eV peak is due to the unoccupied state of the Graphite. Thus, there should be another true mechanism to emit the 3.3-eV electrons. Our next goal will be finding it and is now under progress by using the photoelectron-secondary electron coincidence spectroscopy.

[1] R. F. Willis, B. Fitton, and G. S. Painter, Phys. Rev. B **9** (1974) 1926.

[2] S. Tanaka M. Matsunami and S. Kimura, Phys. Rev. B **84** (2011) 121411(R) .

BL8B

Interface Electronic Structure of Diindenoperylene on Cu(111)

S. Kera[1], K. Kato[1], K. Yonezawa[1], K. Sato[1], Y. Liu[1], N. Ueno[1] and T. Hosokai[2]

[1]*Graduate School of Advanced Integration Science, Chiba University, Chiba 263-8522, Japan*

[2]*Faculty of Engineering, Iwate University, Morioka 020-8551, Japan*

Electric property of organic semiconductor materials is dominated by the density-of-states at the band gap and wavefunction spread of the electronic states. The molecule-substrate interaction crucially influences electronic and geometric properties at the interface [1]. The adsorption geometry of large π-conjugated molecules on metal surfaces, therefore is one of the key targets to understand the variety of peculiar interface properties. Diindenoperylene (DIP: $C_{32}H_{16}$) (inset in Fig 2b) is a typical organic semiconductor. The DIP monolayer (ML) films are prepared on Cu(111) substrate to reveal the interface electronic structure by using angle-resolved ultraviolet photoelectron spectroscopy (ARUPS).

ARUPS spectra were measured at photon incidence angle α=45°, hv=28 eV and T=295 K. The molecules were evaporated onto the Cu(111). The coverage/thickness of the monolayer was confirmed by work function of the densely-packed ML film which shows a clear LEED pattern.

Figure 1 shows the ARUPS of DIP 1ML on the Cu(111). The azimuthal angle (ϕ) dependence is recorded at photoemission angle of θ= 37° by rotating the ϕ_s. The interface states (IS) denoted by B_1, B_2 and B_3 are observed. The features B_1 and B_2 (B_3) would be related to the former LUMO and former HOMO of DIP as reported similarly in PTCDA/Ag(111) and PTCDA/Cu(111), respectively [2]. There is no clear energy-band dispersion for the ISs. The feature B_1 is appeared as a broadened feature and hardly to discuss the origin of electronic state at the present results. On the other hand, the features B_2 and B_3 show a clear angular distribution in the ϕ rotation.

Figure 2(a) shows the photoelectron angular distribution (PAD) of features B_2 and B_3. The PAD of B_2 shows the maximum at around ϕ_s=0°, while B_3 gives the minimum. Fig. 2(b) represents the simulated PAD for the LUMO and HOMO distribution of isolated DIP molecule by using multiple-scattering theory combined with molecular orbital calculation (MS/MO) [3]. The molecule is placed that the molecular longer axis sets in the plane of electric vector (ϕ_m=0°) as seen in Fig. 2(b). The observed PAD of features B_2 and B_3 would be represented by the PAD pattern of HOMO for different molecular azimuthal orientation in the crystal domains. The results of LEED and STM indicate that the ML film consists of at least two different molecular unit cell. Depending on the lattice constant and molecular arrangement the absorption energy would be modified, hence they give the different binding energies. A molecular azimuthal orientation will be analyzed by considering the LEED, STM and simulated PAD. To reveal each orbital character of ISs, a full-spherical map of the PAD is requested to be measured.

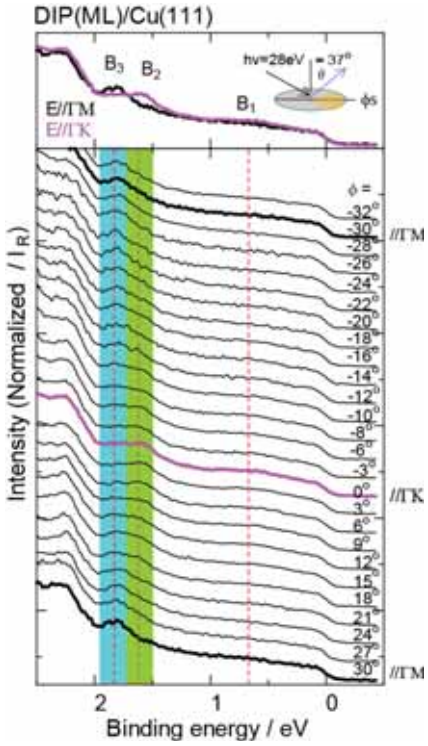

Fig. 1. ϕ dependence of ARUPS for DIP ML film prepared on Cu(111).

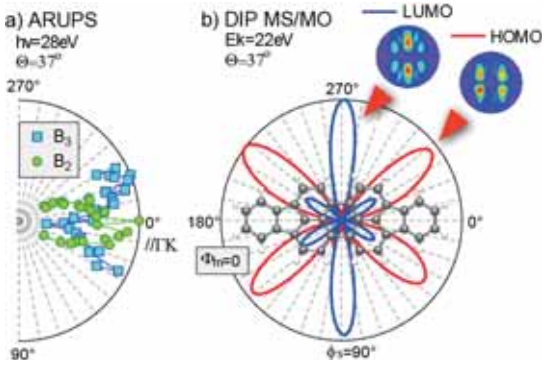

Fig. 2. Observed PAD of features B_2(circles) and B_3(squares) (a) and calculated PAD of LUMO and HOMO distribution by MS/MO (b). Full-spherical PAD images are also shown. The simulated patterns are displayed by slicing the image at θ=37°. Scheme view of DIP molecule at ϕ_m=0 is also shown.

[1] G. Heimel *et al.,* Nature Chem. **5** (2013) 187.

[2] J. Ziroff *et al.,* Phys. Rev. Lett. **104** (2010) 233004.

[3] S. Kera *et al.*, Chem. Phys. **325** (2006) 113.

Role of Oxygen Side Group on Interface State Formation in π-conjugated Organic Molecule/metal System

T. Hosokai[1], K. Yonezawa[2], K. Kato[2], N. Ueno[2] and S. Kera[2]
[1]*Department of Materials Science and Technology, Iwate University, Morioka 020-8551, Japan*
[2]*Graduate School of Advanced Integration Science, Chiba 263-8522, Japan*

Electronic structure of organic/metal (O/M) interfaces is crucial for Organic Electronics, in which charge carrier injection at the interface dominates device efficiency. Therefore, enormous effort has been devoted for understanding the interface electronic structure by using (angle-resolved (AR)) ultraviolet photoelectron spectroscopy (UPS). One remaining issue in this research field is an interface state (IS). In some O/M systems the IS appears unexpectedly near the Fermi level. It has been elucidated that this state is caused by a charge-transfer from metal substrate to the former lowest unoccupied molecular orbital (LUMO) state of the adsorbates. From x-ray standing waves (XSW) experiments on monolayers of perylene compound with acyl groups (PTCDA: $C_{24}H_8O_6$)(Fig. 2)) on noble metal substrates (Au(111), Ag(111) and Cu(111)), it was implied that a shorter bonding distance of the adsorbates onto the substrates may trigger to form the IS [1]. In such case, however, a role of chemical bonding of the side acryl groups to the substrates for the IS is not yet clarified.

To address this issue, we have focused diindenoperylene (DIP: $C_{32}H_{16}$) (Fig. 2), a perylene compound consisting of only carbon and hydrogen atoms. From XSW we confirmed that the bonding distance of DIP to noble metal substrates was similar to that of PTCDA [2]. Here we performed ARUPS study of DIP monolayer (ML) films deposited on Ag(111) and Cu(111), and also on polycrystalline-Ag and -Cu surfaces.

ARUPS spectra were measured at photon incidence angle α=45°, *hv*=28 eV and 40 eV and T=295 K. The molecules were evaporated onto each substrate. The ML formation was confirmed by saturation of the work function shift.

As shown in Fig. 1, the ML spectrum of DIP on Ag(111) and Cu(111) shows some spectral features (as denoted to A_1 – A_4 for Ag(111) and B_1 – B_3 for Cu(111)) distinct from theoretical one or multilayer (island) film spectrum (b_2). This is a direct evidence of IS formation on Ag(111) and Cu(111) surfaces. Notably, such ISs are also seen on polycrystalline surfaces, suggesting the importance of IS in organic devices employing those metal electrodes and DIP.

Figure 2 shows comparison of the energy level alignments of DIP and PTCDA on Ag(111) and Cu(111). ISs are located at nearly the same positions for both molecular films. This clearly indicates that the O-atoms are not necessarily required to form the IS. A strong interaction between the π-conjugated carbons and substrate atoms, which may be realized by a short bonding distance, can be also a key for the IS.

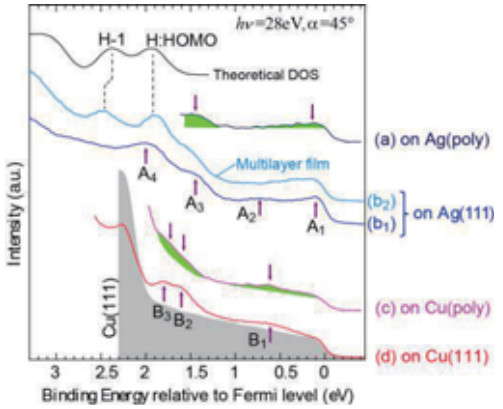

Fig. 1. Valence band structure of DIP ML on Ag(poly) (θ=0°) (a), Ag(111) (θ=40°) (b_1), Cu(poly) (θ=0°) (c) and Cu(111) (θ=37°) (d). Multilayer (island) film (1 nm) of DIP/Ag(111) (θ=30°, *hv*=40eV) (b2). A calculated density-of-state (DOS) of DIP molecule based on B3LYP/6-31G(d) is also shown at the top.

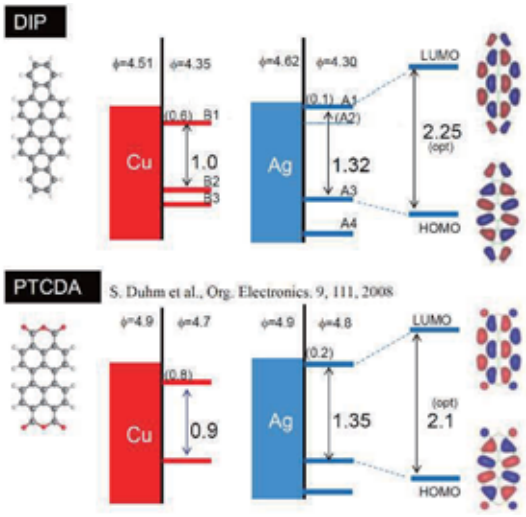

Fig. 2. Energy-level alignment of DIP/Ag(111) and Cu(111) systems compared with PTCDA from ref [1]. The energy levels of multilayer films and orbital pattern of HOMO and LUMO are depicted at the right-hand side, respectively.

[1] S. Duhm *et al.*, Org. Electronics, **9** (2008) 111.
[2] C. Bürker *et al.*, submitted.

BL8B

Quantitative Analysis of Anisotropic Molecular Orientation of Pentacene Thin Film

K. K.Okudaira, T. Ishii and N. Ueno

Association of Graduate Schools of Science and Technology, Chiba Univererity, 1-33 Yayoi-cho Inage-ku, Chiba 263-8522, Japan

In recent years, organic semiconductor materials have proven to be one of the most popular materials used in the fabrication of thin-film transistor The performance of organic-TFT such as the field-effect mobility depends not only on the molecular structure of the semiconducting films but also the degree of molecular orientation, since charge transport in organic materials is realized by π-π interactions between molecules through the hopping mechanism. The anisotropic mobility could be useful in isolating neighboring components so as to reduce cross-talk. We apply a method to control both the molecular and crystal orientation of organic semiconductors, producing films with strong anisotropy. The anisotropic orientation of pentacene (Pn) film can be obtained by evaporating pentacene on the uniaxially oriented PTFE thin films onto the uniaxially polished Cu plate To obtain the quantitative analysis on the molecular orientation; we compare observed take-off angle dependence of π band and calculated one by the independent-atomic-center (IAC)/MO approximation [1].

ARUPS measurements were performed at the beam line BL8B of the UVSOR storage ring at the Institute for Molecular Science. The take-off angle (θ) dependencies of photoelectron spectra were measured at incident angle of photon (α) = 45° with the photon energy (hν) of 40 eV. Pentacene was evaporated to a final thickness of 10 nm on the uniaxially PTFE(5nm)/Cu (Pn(10nm)/ PTFE (5nm)/ Cu).

We observed take-off angle (θ) dependence of HOMO peak in UPS of (Pn(10nm)/ PTFE (5nm)/ Cu). Figure 1 shows the θ dependence of photoelectron from HOMO band with the parallel and perpendicular condition Under the parallel and perpendicular condition, the polarization plane of incidence photon is parallel and perpendicular to the direction of the groove of Cu plate, respectively. the θ dependences with parallel condition have a sharp maxima at θ= 65°. On the other hand, with the perpendicular condition, the θ dependence of HOMO band does not show a strong θ dependence. (θ for the maximum of is lower than that with parallel condition).

Figure 2 (a) and (b) show the calculated θ-dependence of HOMO peak for two geometries. With the geometry (1) and (2), the polarization plane is parallel and perpendicular to the a-axis of bulk phase pentacene crystal, respectively. For the geometry (1). the calculated θ-dependence of HOMO

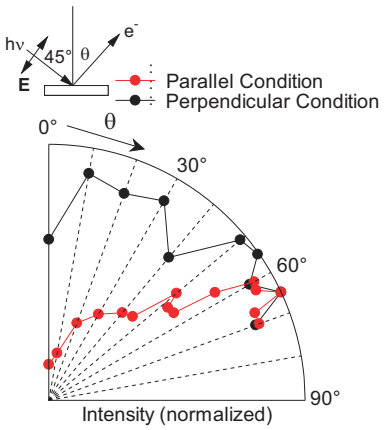

Fig. 1. Take-off angle (θ) dependences of photoelectron intensities of HOMO peak of n(10nm)/ PTFE (5nm)/ Cu) with parallel (●) and perpendicular condition (●).

peak shows a maximum of θ =70°. It is similar with observed one with parallel condition. On the other hand, for the geometry (2) the calculated θ-dependence of HOMO peak shows a maximum of θ =40°, which is lower than that for the geometry (1). From the comparison between observed and calculate ones,. it can be expected that pentacene molecules have the anisotropic molecular orientation on uniaxial PTFE film, where the a-axis of pentacene crystal is parallel to the direction of groove of Cu plate.

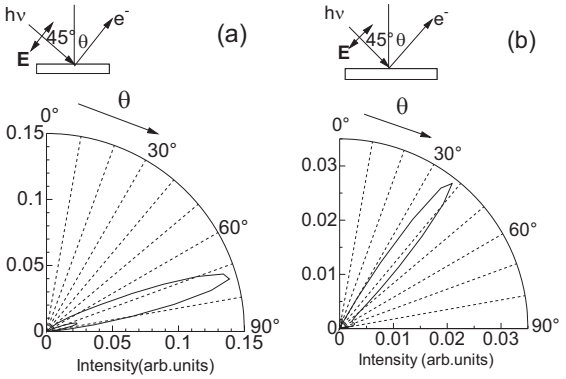

Fig. 2. Calculated θ-dependence of HOMO peak for two geometries. where the polariaion plane of incidence photon is parallel (a) and perpendicular (b) to the a-axis of bulk phase pentacene crystal.

[1] S. Hasegawa *et al*., Phys. Rev. B **48** (1993) 2596.

BL8B

Ultraviolet Photoelectron Spectroscopic Study on the Electronic Structure of the L-cysteine Ad-layers on the Noble Metal Surfaces

K. K. Rasika, Y. Nakayama and H. Ishii
Center for Frontier Science, Chiba University, Chiba 263-8522, Japan

In recent years the possibility to use proteins in bioelectronic devices has attracted much attention. In order to use proteins for bioelectronic applications, it is essential to investigate on the electronic structures of amino acids as the building blocks of proteins to elucidate functionality such as transport properties, adsorption properties, interface, and so on. As the initial step, we selected L-cysteine from the amino acids for the investigation, because it has been reported that the cysteine with its sulfanyl as a promising candidate for bioelectronics [1].

In the present study, we systematically elucidated the electronic structure at the interfaces of L-cysteine over layers and the noble metal surfaces Au(111), Ag(111), and Cu(111) by means of ultraviolet photoelectron spectroscopy (UPS) at BL8B.

Figure 1 shows the thickness-dependent UPS spectra of L-cysteine on (a) Ag(111), (b) Au(111), and (c) Cu(111) at photon energy of 28 eV. In each figure, on the left, the secondary energy cutoff (SECO) is shown on a magnified scale. On the right, the region between Fermi level of the metal substrate and the HOMO of the L-cysteine measured with relatively small energy step is also shown.

It was observed that the electronic structures of the L-cysteine thin films are different from each other and also from that of the L-cysteine thick film, which indicates strong dependence on the kind of substrate. On the thin films, a new structure appears in between Fermi level and the HOMO of the L-cysteine and the structure may be due to bonding of S 3*sp* orbital with Ag 4*d*, Au 5*d*, and Cu 3*d* states for each substrate, respectively. Further, the peak at ~5 eV for thin films shifts to the higher binding energy (e.g., Au by ~ 0.3 eV) (Fig.1., dotted line), may be due to the interaction of O 2*sp* orbital with metal substrates. The maximum SECO shifts were estimated to be 0.46, 0.83, and 1.01 eV to a higher binding energy for Ag, Au, and Cu, respectively. The direction of the shifts corresponding to a net transfer of negative charge from the cysteine to the substrates and the low value for Ag may be due to relatively large energy difference of S 3*sp* and Ag 4*d* states (a weak Ag-S bonding) [2].

Despite the difference in electronic structure for thin films, the electronic structure of thick film is identical for each substrate. Thus, for the thick films, photon energy-dependent UPS spectra were measured in the range of 20-120 eV. The results are shown that the top of valance band (VB) has a different origin from the other structure. By considering the results of Ogawa *et al.* [2], and DV-Xα molecular orbital calculation, it is attributed that the top of VB is originated by sulfur.

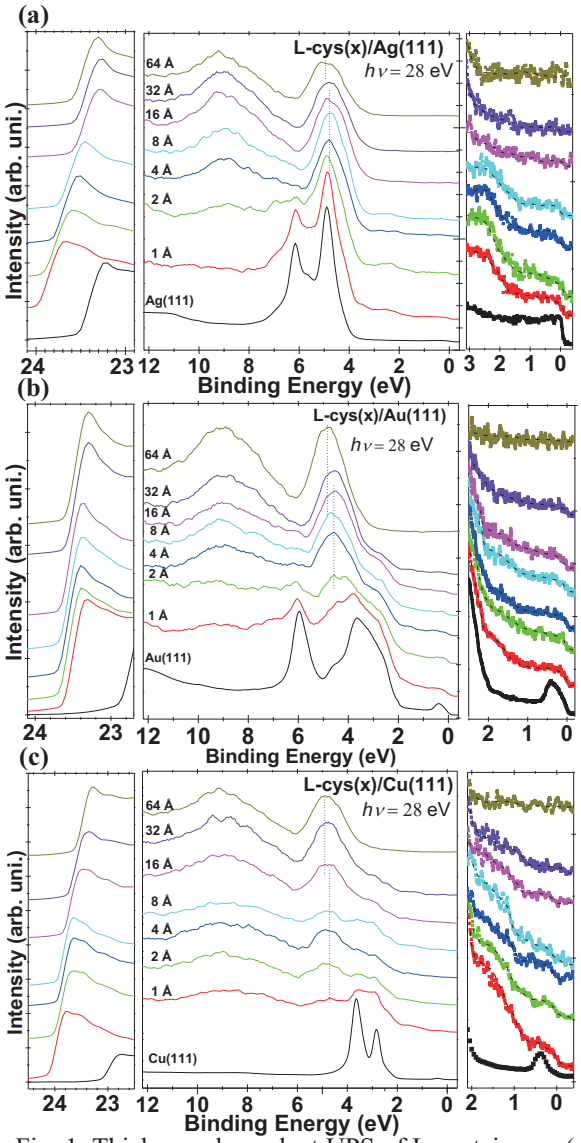

Fig. 1. Thickness-dependent UPS of L-cysteine on (a) Ag(111), (b) Au(111), and (c) Cu(111) at photon energy of 28 eV. In each figure, on the left, the SECO is shown on a magnified scale. On the right, it is shown that the region between Fermi level of the substrate and the HOMO of the cysteine, which was measured with relatively small energy step and the dashed curves are plotted as a guide for eye.

[1] L. Willner and E. Katz, *Bioelectronics*: *From Theory to Applications* (Wiley-VCH, Weinheim, 2005).
[2] K. Ogawa *et al.*, J. Appl. Phys. **112** (2010) 023715.